Cláudia Sofia Godinho Freitas

B. Sc in Biochemistry

How *Staphylococcus epidermidis* and *Staphylococcus aureus* cope with oxidative and nitrosative stress

Dissertation presented to obtain the Master's Degree in
Biochemistry for Health

Supervisor: Lígia Saraiva PhD, Principal Investigator, ITQB-UNL
Co-supervisor: Sandra Carvalho PhD, Post-doc, ITQB-UNL

September 2018

Cláudia Sofia Godinho Freitas

B. Sc in Biochemistry

How *Staphylococcus epidermidis* and *Staphylococcus aureus* cope with oxidative and nitrosative stress

Dissertation presented to obtain the Master's Degree in
Biochemistry for Health

Supervisor: Lígia Saraiva PhD, Principal Investigator, ITQB-UNL
Co-supervisor: Sandra Carvalho PhD, Post-doc, ITQB-UNL

Jury

President	Pedro Manuel Henriques Marques Matias, PhD
Opponent	Ana Margarida Teixeira Saramago, PhD
Supervisor	Lígia Raquel Mendonça Faria Marques Saraiva Teixeira, PhD

Oeiras

September 2018

From left to right: Lígia Saraiva (supervisor), Margarida Saramago (opponent), Cláudia Freitas, Sandra Carvalho (co-supervisor), Pedro Matias (president of the jury).

November 14th, 2018

How *Staphylococcus epidermidis* and *Staphylococcus aureus* cope with oxidative and nitrosative stress

Acknowledgments

A great many people have directly or indirectly contributed to the execution of this thesis and I could not fail to express them my gratitude.

To my supervisor, Dr. **Lígia Saraiva**, I would like to thank the opportunity to join her research group. Thank you for believing in me and in my work. Thank you also for the support and critical revision of this thesis. Lastly, my heartfelt thanks for caring enough to lecture me and give me solid and candid advices, outside the scope of science, and help me grow not only as a scientist but also as a person. Thank you!

Joining the *Molecular Mechanisms of Pathogen Resistance* lab allowed me to meet incredible people.

Sandra, there are not enough words to express how grateful I am to you. Thank you for taking me under your wing and for helping me every step of the way. Thank you for all the patience and for putting up with me, especially in the early stages, when it seemed like I could not even grasp the concept of sterility! Thank you for all the encouragement, advices, scientific discussions, brainstorms, and for pushing me out of my comfort zone. Thank you for sharing my anxiety while experiences run and for getting ecstatic with me when they worked. Your enthusiasm for science is contagious and definitely an inspiration. Thank you also for you help during the writing process!

Joaninha, thank you for always being available to listen and to help, even though my struggles were not within your area of expertise. Thank you for all the advices you gave me and for trying to ease my uneasiness. Thank you for all the talks and laughs, for your friendship and tenderness. I miss you dearly (even your auntie side).

Lili, my esteemed look-alike, thank you for always having the patience to attend to my million questions and go through old journals and files to help me! Thank you for your companionship and for the endless conversations about lab work which I treasure dearly.

Marquitos, thank you for your friendship and cumplicity! The lab would not be the same without your constant complaining and sighs. Thank you for all the rides home (and elsewhere), and the advices you gave me along the way.

Cátia, thank you for your help with the molecular biology techniques and for all the pep talks. Thank you also for making it impossible to lunch without bursting into laughter! **Patrícia**, thank you for all the kindness you showed me in the short period of time we got to work together, and after.

Dear **Sofs**, sharing this endeavor with you has been a joy. Thank you for being the best partner in crime one could ask for. Thank you for all the friendship and silliness, the great talks and for always being there. Thank you for all the times your molecular biologist-self filled in the gaps of my biochemist-self.

To all of you, thank you for enduring my never-ending curiosity and for indulging me when I sneak up on you in a middle of an experiment wanting to know what it is, what is the method you are using and why. Thank you for making the lab such a fun and friendly place to work in.

To those who guided me in my first steps in the research world, **Rui** and **Susana**, thank you for all the knowledge you passed on to me, which I still keep close to my heart and that have come in handy so many times! I extend the same thanks to the other members of the group, **Cindy**, **Cíntia**, **Cláudia**, and **Rute**. Especially, **Alex**, thank you for still giving me a kind word whenever we cross paths.

Cati, Ricardo e Diogo, thank you for putting up with me since the first day of our Bachelor's degree! Thank you for the rides, the companionship, all the great talks and moments of fun. This journey would not have been the same without you. In particular, **Ricardo**, thank you for all the live concerts on our way home! And to you, **Cati**, thank you for keeping me company in the third floor, especially in the common laminar flow hood!

To my writing companion, thank you for the motivation and advice on future life as a student and a researcher. Thank you for believing in me and reminding me that positive results are not everything. Thank you also for the unsolicited criticism of the visual aspect of my data plots.

Diogo, thank you for all the love and care. Thank you for always being my number one supporter and for listening to me talk endlessly about lab stuff. Thank you for understanding my absences and tight schedule. Life is better with you.

I dedicate this thesis to my **dad**, my biggest love and constant role model. Thank you for always going above and beyond for me. Thank you for always asking how my day was and if my bacteria grew, even though you do not grasp the world I chose.

Abstract

Staphylococcus epidermidis and *Staphylococcus aureus* are predominant colonizers of the human skin and important nosocomial pathogens. These pathogens form biofilms, mainly on implanted medical devices, that are resistant to antibiotics and to the chemicals produced by the host immune system. In particular, professional phagocytes of the innate immunity release toxic reactive oxygen species (ROS) and reactive nitrogen species (RNS) that are highly damaging to pathogens, whose survival depends on their defense mechanisms.

In this work, I have studied how planktonic cells and biofilms of *S. epidermidis* and *S. aureus* survive the damage inflicted by ROS/RNS. To this end, two *S. epidermidis* clinical strains and a *S. aureus* laboratory strain were analyzed. Cells were exposed to oxidative and nitrosative stress, under different growth conditions, and the growth rate of planktonic cells and amount of biofilm biomass was evaluated. Furthermore, the role of two *S. aureus* proteins involved in stress detoxification and repair, namely flavohemoglobin (*hmp*) and repair of iron centers protein (*ric*), was analyzed regarding their contribution to stress survival.

Data showed that the *S. epidermidis* strains are highly resistant to oxidative and nitrosative stress, and that biofilm formation is more compromised when the stresses are applied before biofilm´s establishment. On the contrary, the biofilms of *S. aureus* are more susceptible to these stresses. As for the role of the two *S. aureus* proteins, while deletion of *ric* did not affect the biofilm response to nitrosative stress, inactivation of *hmp* restored the biofilm formation levels similar to those of untreated cells.

Altogether, it is shown that under stress conditions the ability of *S. epidermidis* and *S. aureus* to form biofilms contributes to the survival of the two bacteria. Hence, this work contributed to advance the state-of-the-art regarding the defense mechanisms of two important pathogens against weapons of our immune system.

Keywords: *S. epidermidis*, *S. aureus*, biofilms, oxidative stress, nitrosative stress

Resumo

Staphylococcus epidermidis e *Staphylococcus aureus* são colonizadores predominantes da pele humana e patógenos nosocomiais importantes. Estes patógenos formam biofilmes, principalmente em dispositivos médicos implantados, resistentes a antibióticos e aos químicos produzidos pelo sistema imunitário do hospedeiro. Especificamente, os fagócitos profissionais da imunidade inata libertam espécies reativas de oxigénio (EROs) e espécies reativas de nitrogénio (ERNs) altamente prejudiciais aos patógenos, cuja sobrevivência depende de mecanismos de defesa.

Neste trabalho, estudei a sobrevivência de células planctónicas e biofilmes de *S. epidermidis* e *S. aureus* ao dano infligido pelas EROs e ERNs. Para tal, analisei duas estirpes clínicas de *S. epidermidis* e uma estirpe laboratorial de *S. aureus*. As células foram expostas a stress oxidativo e nitrosativo, sob condições diferentes de crescimento, e a taxa de crescimento das células planctónicas e a biomassa de biofilme produzida foram avaliadas. Ademais, analisaram-se duas proteínas de *S. aureus* envolvidas na destoxificação e reparação de stress, a flavohemoglobina (*hmp*) e a reparadora de centros de ferros (*ric*), quanto ao seu contributo para a sobrevivência ao stress.

Os resultados demonstraram que as estirpes de *S. epidermidis* são altamente resistentes ao stress oxidativo e nitrosativo, e que a formação de biofilme é mais comprometida quando os stresses são aplicados antes do estabelecimento do biofilme. Contrariamente, os biofilmes de *S. aureus* são mais suscetíveis a estes stresses. Relativamente às proteínas de *S. aureus*, enquanto a deleção da *ric* não afetou a resposta dos biofilmes ao stress nitrosativo, inativação da *hmp* restaurou a formação de biofilme a níveis semelhantes aos das células não tratadas.

Assim, é demonstrado que a capacidade de *S. epidermidis* e *S. aureus* para formarem biofilmes contribui para a sua sobrevivência a stress. Consequentemente, este trabalho contribuiu para avançar o estado da arte relativamente aos mecanismos de defesa de dois patógenos importantes contra armas do nosso sistema imunitário.

Palavras-chave: *S. epidermidis*, *S. aureus*, biofilmes, stress oxidativo, stress nitrosativo

Table of Contents

Index of Figures

Index of Tables

List of Abbreviations

A	**ATCC**	American type culture collection
	agr	Accessory gene regulator
B	**bp**	Base-pair
C	**CoNS**	Coagulase-negative staphylococci
	CoPS	Coagulase-positive staphylococci
	CA	Community-acquired
	CFUs	Colony-forming units
	cDNA	Complementary deoxyribonucleic acid
	C_t	Comparative threshold
D	**DNA**	Deoxyribonucleic acid
	Da	Dalton
	dNTPs	Deoxynucleotides
E	***et al.***	From the Latin *et alia*, meaning «and others»
	e.g.	From the Latin *exempli gratia*, meaning «for example»
	eDNA	Extracellular deoxyribonucleic acid
	E.	*Escherichia*
	EPR	Electron paramagnetic resonance
F	**FAD**	Flavin adenine dinucleotide
	Fe-S	Iron-sulfur
G	**GC**	Guanine-cytosine
	G.	Galleria
	Glc	Glucose
	GSNO	S-Nitrosoglutathione
	gDNA	Genomic deoxyribonucleic acid
I	***i.e.***	From the Latin i*d est*, meaning «that is»
	iNOS	Inducible nitric oxide synthase
L	**LB**	Luria-Bertani
M	**MRSE**	Methicillin-resistant *Staphylococcus epidermidis*
	MSSE	Methicillin-sensitive *Staphylococcus epidermidis*
	MRSA	Methicillin-resistant *Staphylococcus aureus*
	MSCRAMMs	Microbial surface components recognizing adhesive matrix molecules
	MCS	Multiple cloning site
N	**NK**	Natural killer cells
	NETs	Neutrophil extracellular traps
	NADPH	Nicotinamide adenine dinucleotide phosphate
	NO	Nitric oxide
	NARSA	Network on antimicrobial resistance in *Staphylococcus aureus*
O	**OD**	Optical density
P	**PSMs**	Phenol-soluble modulins

	PIA	Polysaccharide intercellular adhesin
	Phox	Phagocyte oxidase
	PDB	Protein data bank
	PBS	Phosphate-buffered saline
	PCR	Polymerase chain reaction
Q	**qRT-PCR**	Real-time quantitative reverse polymerase chain reaction
R	**ROS**	Reactive oxygen species
	RNS	Reactive nitrogen species
	RIC	Repair of iron centers protein
	rpm	Rotations per minute
	RNA	Ribonucleic acid
S	***S.***	*Staphylococcus*
	Spp.	Species
	SCC*mec*	Staphylococcal cassette chromosome *mec*
	sarA	Staphylococcal accessory regulator
	σ^B	Sigma factor B
	SOD	Superoxide dismutase
	Spm	Spermine
	SOE-PCR	Splicing by overlap extension polymerase chain reaction
	SD	Standard deviation
T	**TSB**	Tryptic soy broth
	TSA	Tryptic soy agar
U	**USA**	United states of America
	UV	Ultraviolet

Somewhere, something incredible is waiting to be known.

- Carl Sagan

I. Introduction

I.1. *Staphylococcus epidermidis*

Staphylococcus epidermidis (Figure I.1) is a Gram-positive spherical bacterium, measuring around 1 µm in diameter [1], with a low GC content (~32%). This microorganism is capable of forming biofilms and of growing in environments either fully oxygenated or with low oxygen concentrations, although it grows best in the first condition (*i.e.*, it is a facultative anaerobe).

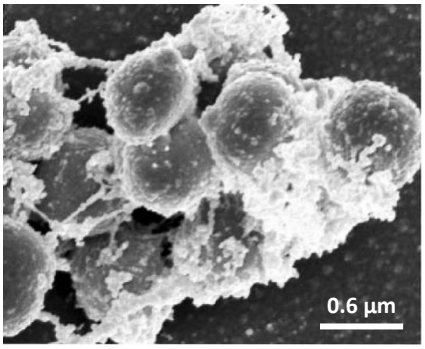

Figure I.1. Scanning electron image of *S. epidermidis* magnified 25 000-times. Adapted from Vuong, C. *et al.* (2004).

S. epidermidis was first identified in 1880 by Ogston [2] and, at first, it was known as *S. albus* (from the Latin *albus*, meaning "white"), by contrast with *S. aureus* (from the Latin *aureus*, meaning "golden"), due to its lack of pigmentation. Currently, *Staphylococcus* spp. are grouped based on the production of coagulase rather than of pigments (Figure I.2). *S. epidermidis* belongs to the heterogeneous group of coagulase-negative staphylococci (CoNS) while *S. aureus* is the most notorious representative of coagulase-positive staphylococci (CoPS).

S. epidermidis is a common colonizer of the skin and mucous membranes of humans and animals [3]. In humans, it is one of the most predominant and persistent staphylococci isolated from the skin, namely from the nares, axillae, head, legs and arms [4]. Since CoNS typically do not produce aggressive virulence factors or cause infections in their hosts [5], they were regarded as non-pathogenic for a long time. However, their pathogenic potential began to be recognized in the late 1980s and,

currently, they constitute major nosocomial pathogens. *S. epidermidis* is the species most commonly associated with CoNS infections, and its emergence as an important nosocomial pathogen is associated with demographic and medical alterations. Namely, the groups susceptible to *S. epidermidis* infections include premature neonates, the elderly, immunosuppressed individuals, and individuals with indwelling or implanted medical devices [5], which became pivotal in modern medicine.

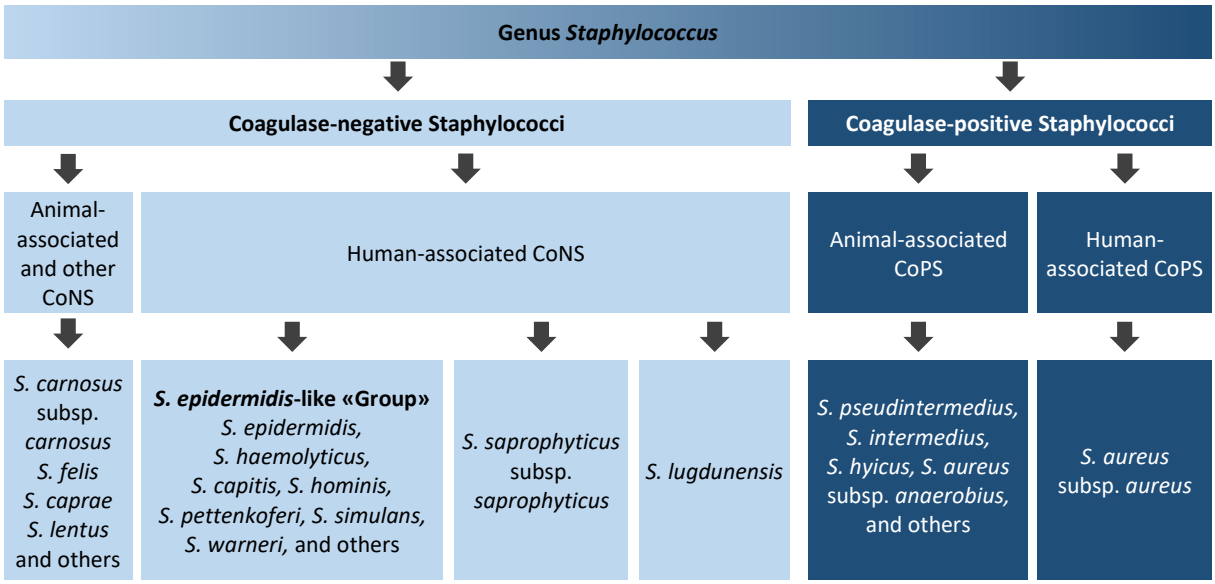

Figure I.2. Clinical and epidemiological schema of staphylococcal species based on the categorization of coagulase as a major virulence factor, and its impact on human health. Adapted from Becker, K. *et al.* (2014).

As previously mentioned, *S. epidermidis* does not produce a wide range of aggressive factors. Virulence factors consist of bacterial products or strategies that enable bacteria to colonize and invade a host, evade its immune defenses, acquire nutrients from and spread within the host [6]. Virulence factors are diverse in origin and function and include toxins, enzymes, cell surface proteins and carbohydrates, among others. These factors can either be encoded in the bacterial chromosome or in mobile genetic elements, such as plasmids and pathogenic islands [3]. Those encoded by mobile genetic elements can be spread between bacteria through horizontal gene transfer.

To colonize the human skin, *S. epidermidis* must adhere to it and cope with mechanical stress, high salt concentrations, osmotic pressure and evade its immune defenses (described further in section I.4.1) [6]. The mechanisms that enable *S. epidermidis* to endure these conditions also prove beneficial during infection, highlighting the opportunistic and accidental nature of the infections it causes. While *S. aureus* produces a vast repertoire of toxins, *S. epidermidis* virtually only produces phenol-soluble modulins (PSMs) [7]. PSMs are short, amphipathic, α-helical peptide toxins produced by most staphylococcal strains, and have multiple functions including promotion of inflammatory

responses, contribution to biofilm structuring and detachment, and antibacterial and cytolytic activities (towards leukocytes and other cell types) [8, 9].

Moreover, antibiotic resistance has emerged among *S. epidermidis* strains which may act a reservoirs of antibiotic resistance genes [6]. Most clinical isolates of *S. epidermidis* carry the staphylococcal cassette chromosome *mec* (SCC*mec*), a complex mobile genetic element that encodes methicillin resistance and that might also carry other virulence factors and confer resistance to other antibiotics [10, 11]. Thus, treatment of infections caused by *S. epidermidis* is a difficult endeavor due to the combination of multiple resistance to antibiotics and its distinctive ability to form biofilms.

I.1.1. *Staphylococcus epidermidis* RP62A and 1457

Two clinical strains of *S. epidermidis* were used in this work: *S. epidermidis* RP62A (ATCC 35984) and *S. epidermidis* 1457. The strain RP62A was isolated by Christensen and colleagues during the 1979 – 1980 outbreak of *S. epidermidis* sepsis associated with intravascular catheters, which took place in two hospitals of Tennessee, USA [12]. This is a methicillin-resistant *S. epidermidis* (MRSE) strain and a strong biofilm producer, whose complete genome sequence was determined in 2005 by Gill and colleagues [13].

Strain 1457 was isolated in 1992 by Mack and colleagues from a patient with an infected central venous catheter [14]. This is a methicillin-sensitive *S. epidermidis* (MSSE) strain [15] and a strong biofilm producer that has been widely used as a model for biofilm studies. Unlike many *S. epidermidis* strains (including RP62A), 1457 is amenable to genetic manipulation and its complete genome sequence was determined in 2017 by Galac and colleagues [16].

I.2. *Staphylococcus aureus*

Staphylococcus aureus (Figure I.3.) is a Gram-positive, spherical bacterium of approximately 1 µm of diameter, that forms biofilms. This bacterium was first isolated in 1882 by Ogston [17], and named *Staphylococcus aureus* (from the Greek *staphyle*, meaning “bunch of grapes”, and from the Latin *aurum*, meaning “gold”) due to its appearance of golden cocci which tend to cluster like grapes.

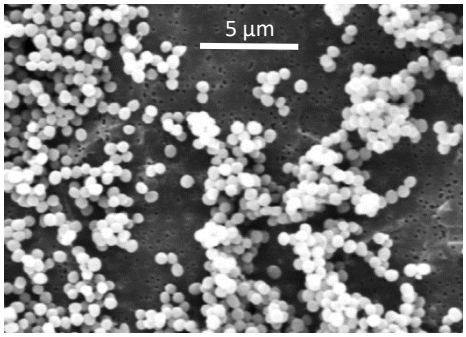

Figure I.3. Scanning electron image of *S. aureus*, magnified 12 000-times. Adapted from Bui, L. *et al*. (2015).

Approximately 30% of the human population is colonized by *S. aureus* [18], which preferentially colonizes the anterior nares but is also capable of colonizing other areas of the body such as the skin, mucous membranes and the gastrointestinal tract [19, 20]. This bacterium is also a major opportunistic pathogen and causes a wide range of infections, ranging from mild to life-threatening, including bacteremia, infective endocarditis and osteoarticular, skin, soft tissue and medical device-related infections [18].

The infections caused by *S. aureus* are often chronic which has been associated with the ability of this pathogen to form biofilms (see below) and persister cells. Persisters are non-growing cells that occur as a sub-population of phenotypic variants, which are highly resistant to antimicrobial agents due to their reduced cellular activity [21]. The mechanism underlying the formation of persisters in *S. aureus* remains to be fully elucidated.

Furthermore, *S. aureus* is the cause of major health concerns to the emergence of strains resistant to multiple antibiotics. Methicillin was developed due to the need of new antimicrobial agents to treat infections caused by strains of *S. aureus* resistant to penicillin [22]. Nonetheless, shortly after its introduction, methicillin-resistant strains started to emerge. At first, infections related to methicillin-resistant *Staphylococcus aureus* (MRSA) were restricted to hospitals and similar settings, but eventually started to appear in the community. MRSA strains are often resistant to multiple antibiotics and isolates resistant to vancomycin, an antibiotic of last resort to treat MRSA, have already been reported [20, 22].

I.3. Biofilms of *Staphylococcus epidermidis* and *Staphylococcus aureus*

The infections caused by *S. epidermidis* and *S. aureus* are associated with their ability to form biofilms on host tissues and abiotic surfaces, such as those of implanted medical devices (*e.g.:* catheters, prostheses, cosmetic implants and pacemakers) [23]. Implanted medical devices increase the

risk of infection by providing a break in the skin barrier, which facilitates the access of potential pathogens on the skin surface to the bloodstream. Indeed, prosthetic infections usually arise from contamination during surgery [24].

Biofilms are generally defined as a sessile bacterial community, in which cells are attached to each other and to a surface and embedded in a self-produced polymeric extracellular matrix composed of polysaccharides, proteins and extracellular DNA (eDNA) [23, 25]. Three main stages can be distinguished in the process of biofilm development: initial attachment, maturation and dispersal (Figure I.3) [23, 24, 26]. After insertion, implants quickly become coated with host proteins, which facilitates the attachment of *S. epidermidis* and *S. aureus* through adhesins like microbial surface components recognizing adhesive matrix molecules (MSCRAMMs), that bind fibrinogen, fibronectin and collagen [24, 26]. During maturation, biofilm accumulates due to intercellular aggregation and production of the extracellular matrix. Finally, cells within the biofilm can detach and return to their planktonic state. Biofilm dispersion leads to bacteria dissemination, which can result in biofilm establishment in a secondary site in the host and represents a potential source of chronic infection and septic shock [6, 26]. The main biofilm disruption strategy used by staphylococci involves the production of extracellular enzymes, namely proteases and nucleases, and PSMs which exhibit surfactant-like properties [24, 26].

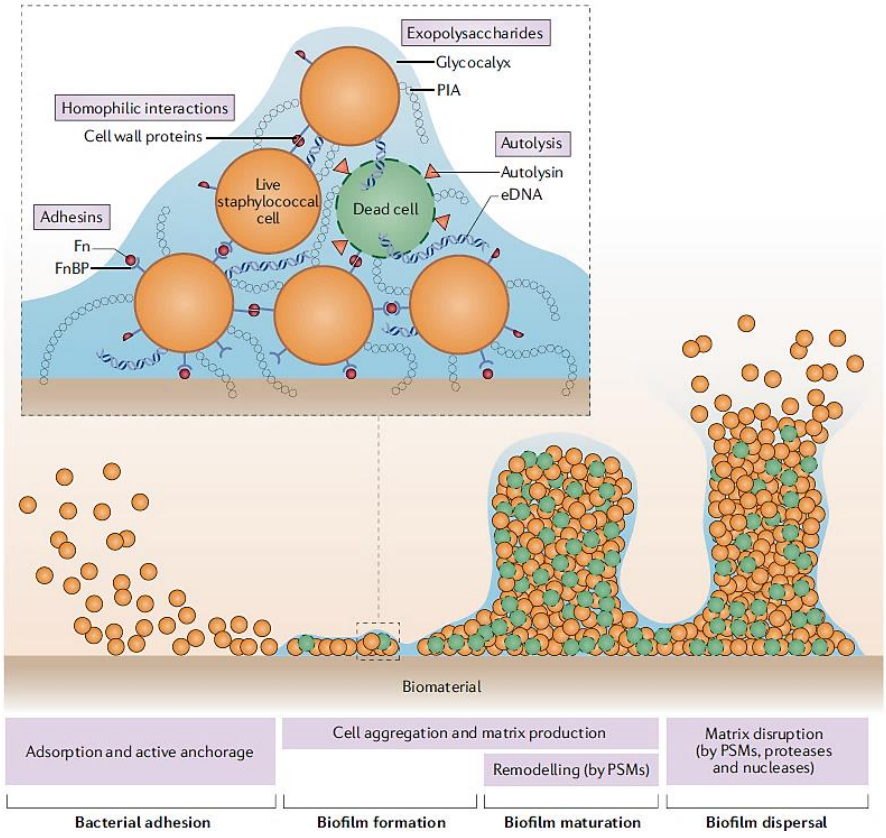

Figure I.4. Stages of staphylococcal biofilm formation. Three main stages can be identified during the biofilm development of staphylococci: initial attachment, maturation and dispersal. From Arciola, C. *et al.* (2018).

Biofilm development in *S. epidermidis* and *S. aureus* is controlled by an intricate and overlapping network of regulatory systems, including the accessory gene regulator (*agr*) system, the staphylococcal accessory regulator (*sarA*), the sigma factor B (σ^B) and the SaeRS two component system [23, 25, 26].

One of the major components of the biofilm matrix of *S. epidermidis* and *S. aureus* is the polysaccharide intercellular adhesin (PIA), a poly-β(1-6)-*N*-acetylglucosamine [26]. Since the enzymes necessary to synthesize PIA are encoded by the *ica* operon [24, 26], these biofilms are designated *ica*-dependent. However, some strains are capable of forming *ica*-independent biofilms, whose matrices are mainly composed of proteins and eDNA that contribute to the intercellular adhesion in the absence of PIA [23, 24, 26]. Therefore, biofilm composition varies among strains of *S. aureus* and *S. epidermidis* and the same strain may exhibit multiple mechanisms for biofilm formation [23].

In the biofilm state, cells exhibit different phenotypic traits from their planktonic counterparts (*i.e.,* free floating cells), namely regarding growth, gene expression and protein production [25, 26]. For instance, the protective biofilm matrix acts as a diffusion barrier to antimicrobial agents and immune effectors, such as phagocytes, which exhibit "frustrated phagocytosis" (*i.e.,* difficulty in engulfing the biofilm due to its size and/or density of the extracellular matrix) [24, 26]. Cells in biofilms display a transient state of resistance to antibiotics and the host immune system, which is reverted once they reenter the planktonic state [26]. Due to the intrinsic resistance of biofilms, infections associated with these are difficult to treat and refractory to antimicrobial therapy. Biofilm-related infections of implanted medical devices usually require removal and replacement of the device and prolonged antibiotic therapy [24, 25]. Moreover, higher rates of mutagenesis and horizontal gene transfer have been detected in biofilms, compared to planktonic growth, which favors the emergence of antibiotic resistance [27, 28].

I.4. Host defenses: the immune system

To preserve its integrity, the host requires defense mechanisms to protect itself from pathogens. This protection is provided by the immune system which can be divided into two parts: the innate immune system and the adaptive immune system. However, even prokaryotes, which do not have a proper immune system, have defense strategies against external threats, such as bacteriophages and exogenous nucleic acids [29, 30].

The innate immune system is phylogenetically older than adaptive immunity [31] and is present in many organisms, such as animals [31-36], plants [37, 38] and insects [39, 40] (recent data also suggest the

existence of innate immunity in fungi [41]). Briefly, it is based on pathogen recognition by receptors that bind microbial structures, which are often common to classes of pathogens [31, 42].

On the other hand, adaptive immunity is only found in vertebrates, and is based on receptors that undergo somatic recombination of gene segments, resulting in higher specificity [31, 42]. The key components of our adaptive immune system, such as lymphocytes, antibodies and specialized lymphoid tissues, evolved in jawed fish about 360 million years ago [31, 42, 43].

The innate immune system constitutes the first line of defense whereas adaptive immune responses take longer to develop (Figure I.5). Although both branches of immunity fulfill different roles, they are strongly interconnected. Innate immunity performs three essential functions: (1) early prevention, control and elimination of infection, (2) elimination of damaged and dead cells and initiation of tissue repair, and (3) stimulation and enhancement of adaptive immune responses [31, 44]. Adaptive immunity mounts more specific responses at later stages of infection and generates immunological memory [31, 44].

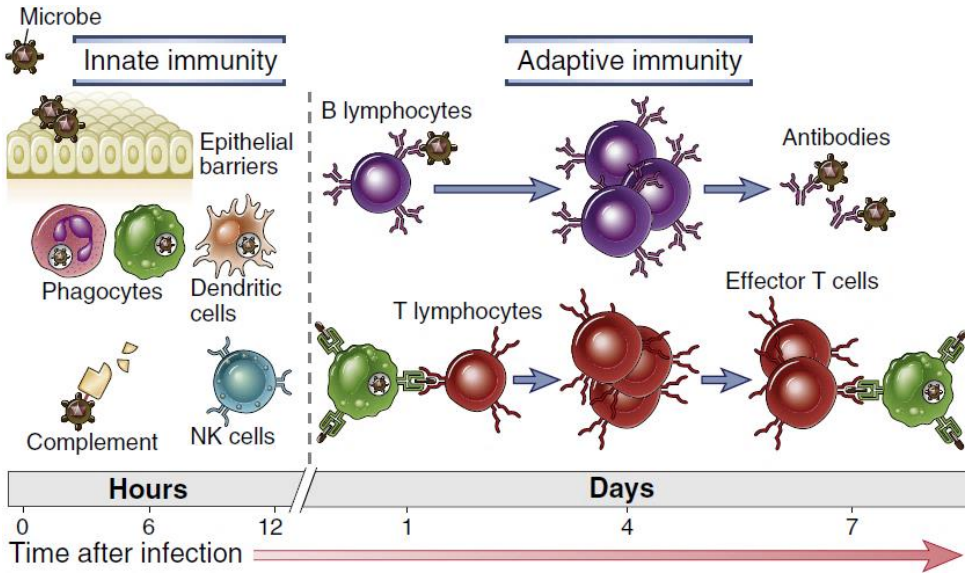

Figure I.5. Time frame and components of innate and adaptive immunity. Adapted from Abbas, A. *et al*. (2014).

I.4.1. Innate immune responses

The innate immune system is composed of several cellular and biochemical components such as physical and chemical barriers (*e.g.*: skin, epithelia, antimicrobial peptides), humoral effectors (*e.g.*.: complement system, lysozyme, cytokines, lactoferrin), and cells (*e.g.*.: phagocytes, NK cells, innate lymphoid cells) [31, 32, 45].

As barriers, the skin and epithelia establish important initial defenses against pathogens (Figure I.6), by isolating the internal environment from the exterior. They are composed of tightly packed cells, which strongly prevents the transition of microbes. The skin surface is composed of dead keratinized cells which are continuously shed, thus removing attached bacteria. Pathogens that are able to bypass these defenses come in contact with other immunological defenses at the epidermidis, such as Langerhans cells (skin-resident dendritic cells) [6]. However, insertion of medical devices such as catheters provides a break in these barriers, which allows pathogens on the skin surface to evade the defense mechanisms mentioned.

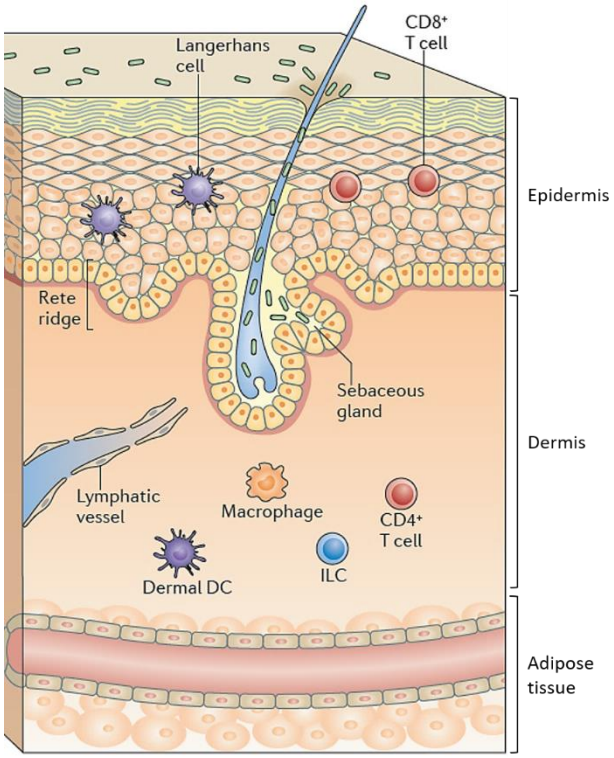

Figure I.6. Scheme of the human skin histology and immune defenses. Adapted from Pasparakis, M. *et al.* (2014).

Phagocytes are cells dedicated to ingesting and killing pathogens, although they also participate in other immune processes and in tissue repair. The major phagocytes are neutrophils and monocytes-macrophages.

Neutrophils are the most abundant leukocytes in circulation and are typically the first to respond in cases of inflammation [31]. Neutrophils can kill microbes through several mechanisms, both intra- and extracellularly, through phagocytosis, release of antibacterial proteins, and formation of neutrophil extracellular traps (NETs) [46]. NETs are web-like structures composed of DNA and proteins, which immobilize pathogens, preventing their dissemination and facilitating their subsequent phagocytosis [47]. Neutrophils are short-lived: they circulate in the blood from a few hours to a few days and, after migrating to the tissues in response to infection, they only survive for one to two days [47].

Monocytes are also circulating leukocytes, albeit less numerous and longer lived than neutrophils [6]. Monocytes are actively recruited into tissues to sites of infection, where they maturate into macrophages, which have a higher phagocytic capacity [6, 31, 48]. Macrophages can exist freely in circulation or reside in tissues and ingest pathogens and dead host cells (tissue homeostasis). Macrophages secrete several cytokines, which promote the recruitment of other leukocytes to the site of infection and also tissue repair (by stimulating angiogenesis and fibrosis) [31, 48].

Phagocytosis is a complex process which progresses in sequential steps (Figure I.7). Binding of pathogens to specific receptors on the phagocyte surface activates several signaling pathways, which result in cytoskeleton rearrangement and membrane remodulation at the site of contact. After the pseudopods merge, the vesicle thus formed (the phagosome) splits from the membrane, and moves towards the center of the cell, where it maturates into the phagolysosome. This maturation process involves a series of membrane fusion and fission events with lysosomes and endosomes. The phagolysosome constitutes a highly acidic (pH below 5) and hydrolytic compartment, where the pathogen is killed. [49-51]

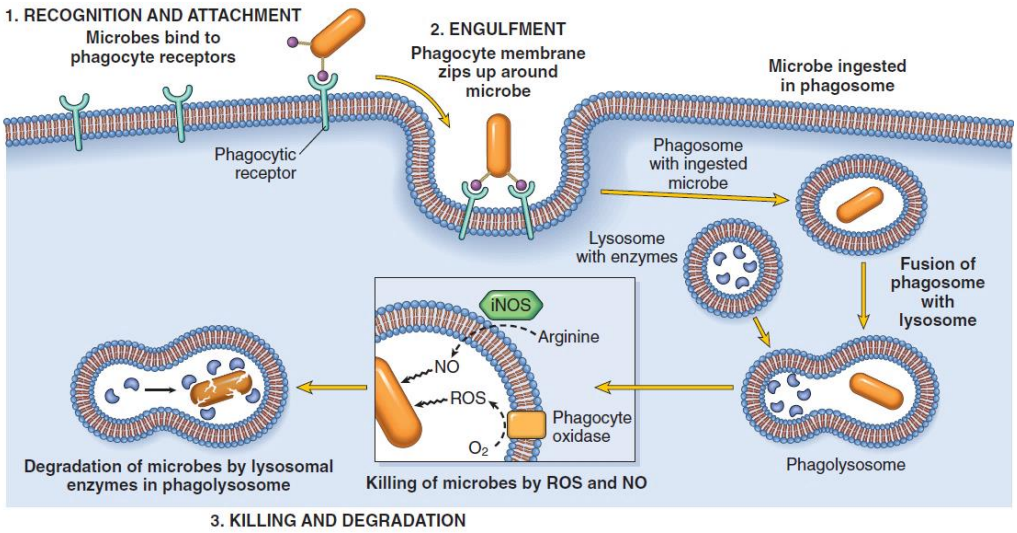

Figure I.7. Sequential steps of microbial phagocytosis. iNOS, inducible nitric oxide synthase; NO, nitric oxide; ROS, reactive oxygen species. From Aderem, A. (2003).

Elimination of phagocytosed pathogens can occur through several mechanisms, which involve mainly reactive oxygen species (ROS), reactive nitrogen species (RNS) and proteolytic enzymes [31, 52]. The main sources of ROS and RNS in phagocytes are the enzymes NADPH oxidase (also known as phagocyte oxidase, Phox) and inducible nitric oxide synthase (iNOS), respectively [52, 53]. Both enzymes are expressed in neutrophils, monocytes and macrophages (albeit neutrophils produce higher

amounts of ROS while macrophages produce higher amounts of RNS) and are dependent on NADPH and oxygen [53].

ROS production occurs during the respiration burst, mainly via Phox, a membrane-bound enzyme which converts molecular oxygen to the superoxide free radical (O_2^-), with the concomitant oxidation of NADPH (Scheme I.1). The superoxide free radical is later converted to hydrogen peroxide (H_2O_2), by the cytosolic enzyme superoxide dismutase (SOD), and gives rise to other ROS.

$$NADPH + 2O_2 \longrightarrow NADP^+ + 2O_2^- + H^+$$ **(Scheme I.1)**

The cytosolic and dimeric enzyme iNOS catalyzes the oxidation of L-arginine, yielding L-citrulline and the gaseous nitric oxide free radical ($NO^\bullet$). $NO^\bullet$ can react with O_2^- and originate species with even more deleterious effects (Figure I.8).

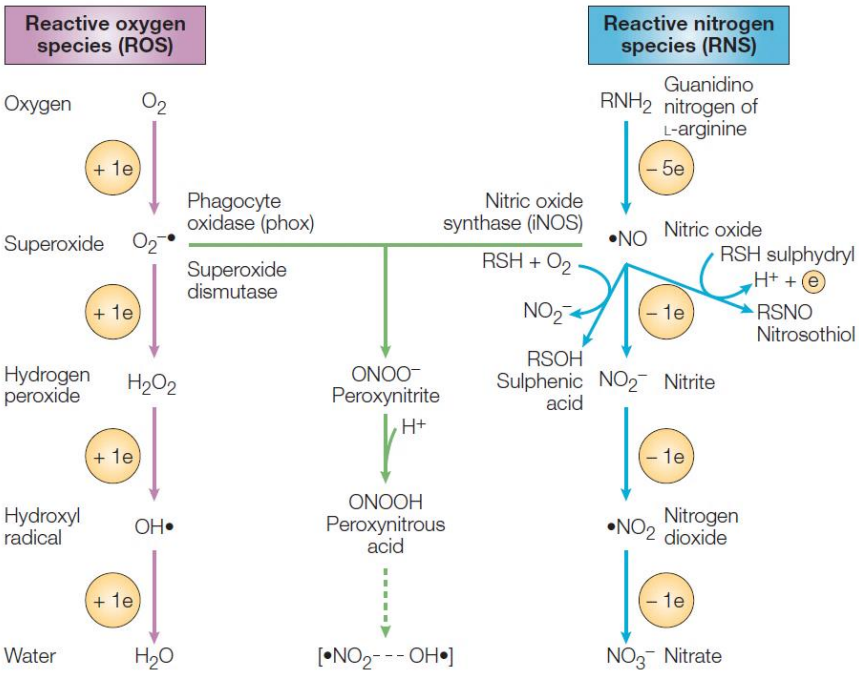

Figure I.8. Production of ROS and RNS in mammalian cells, and the intermediate species that result from their combined chemistry. From Fang, F. (2004).

ROS and RNS constitute very versatile antimicrobial molecules, since the species that comprise each group exhibit different properties, namely reactivity, stability and biological activity [53]. Therefore, they can interfere with several different microbial targets, including thiols, metal centers (such as iron-sulfur centers), certain amino acid residues, DNA and lipids [6, 53]. ROS-mediated effects include DNA damage (involving intermediates generated by Fenton chemistry), lipid peroxidation and oxidative

modifications of proteins, mainly at cysteine, methionine, tyrosine, phenylalanine and tryptophan residues [6, 53]. On the other hand, RNS-mediated effects include inhibition of DNA replication and bacterial respiration [53].

I.5. Bacterial defenses against the innate immune system

Pathogens have evolved diverse defense strategies to cope with ROS and RNS. These strategies encompass evasion, suppression, enzymatic inactivation, scavenging, iron sequestration, stress responses and repair mechanisms [53]. Detoxification can be achieved by enzymatic conversion of ROS and RNS to less toxic species. ROS-detoxifying enzymes include catalase, that converts H_2O_2 to H_2O and O_2, and superoxide dismutase, that converts $O_2^{-\bullet}$ to H_2O_2 or O_2, whereas the major RNS-detoxifying enzymes consist of respiratory nitric oxide reductases, globins and flavodiiron proteins [53]. The genome of *S. epidermidis* contains genes that encode for catalase, superoxide dismutase, flavohemoglobin and a novel-type of diiron protein, the Repair of Iron Centers (RIC) protein.

I.5.1. Flavohemoglobin

Globins, hemeproteins that bind oxygen in a reversible manner, are found in all three kingdoms of life and exhibit varied functions [54, 55]. A classic globin is characterized by the canonical 3/3 α-helical myoglobin fold, which comprises a heme group surrounded by 8 α-helices [54]. This fold provides the hydrophobic environment required for heme function.

Microbial globins encompass several families, including single-domain globins, truncated hemoglobins and flavohemoglobins. Flavohemoglobins are monomeric proteins of approximately 44 kDa, composed of two domains: (1) a globin-like domain, located at the N-terminal and containing a heme B, and (2) a ferredoxin-NADP+ reductase-like domain, located at the C-terminal and containing binding sites for FAD and NAD(P)H (Figure I.9) [56-58]. The active sites of both the heme and flavin domains are highly conserved in the flavohemoglobin family [58].

Flavohemoglobins catalyze the aerobic conversion of NO to nitrate (Scheme I.2) [56].

$$2NO + 2O_2 + NAD(P)H \longrightarrow 2NO_3^- + NAD(P) + H^+ \qquad \textbf{(Scheme I.2)}$$

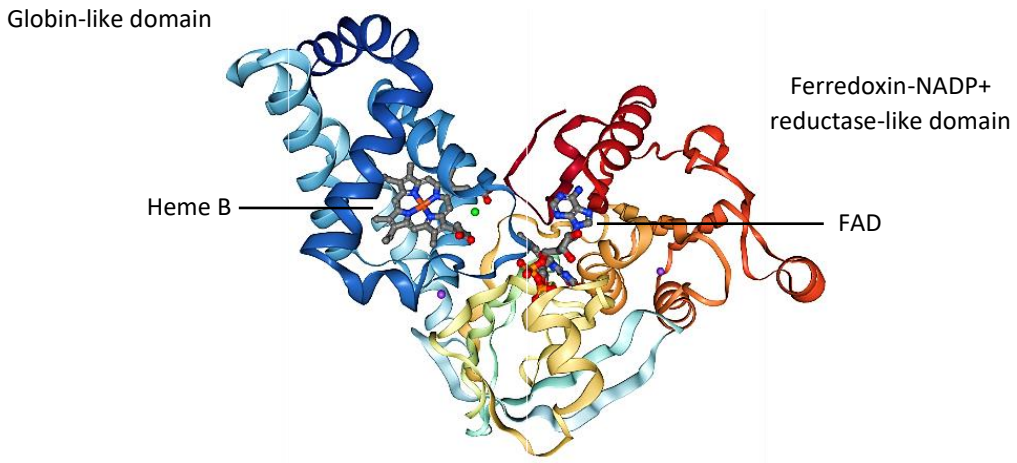

Figure I.9. Crystal structure of the *E. coli* HMP protein (PDB ID: 1GVH), at 2.19 Å resolution. The structure of the staphylococcal homologue has not been determined yet.

The mechanism through which this reaction occurs is still disputed. Two mechanisms have been proposed: (1) the deoxygenation mechanism, which begins with O_2 binding to the ferrous heme, and the (2) nitrosylation mechanism, which begins with NO binding to the ferrous heme [56, 59].

After NO oxidation, the flavohemoglobin undergoes a NAD(P)H-dependent catalytic regeneration [59]. First, NADH reduces the bound FAD, which in turn reduces the heme iron. Oxygen binds tightly to the reduced flavohemoglobin, serving as a substrate for another oxidation reaction. On the other hand, in mammalian globins regeneration of the ferrous heme is much slower and depends on cellular reducing agents [59].

Under anaerobic conditions, flavohemoglobins have also been observed to catalyze the reduction of NO to N_2O. This reaction is much slower and occurs at approximately 1% of the rate of the oxidation of NO to NO_3^- [59].

There are several experimental evidences supporting the role of flavohemoglobins in NO detoxification. For instance, the expression levels of the encoding gene *hmp* are up-regulated by NO and nitrosating agents, and null mutants of *hmp* are hypersensitive to nitrosative stress [56, 57]. Moreover, no other physiological role has been established for flavohemoglobins.

1.5.2. Repair of Iron Centers (RIC) Protein

The *ytfE* gene of *E. coli* sparked interest when it was observed, in 2005, that its transcription is highly induced (≈ 55-fold increase) in *E. coli* K-12 cells grown anaerobically and exposed to NO gas [60]. Since then, transcription of *ytfE* has also been observed to be induced in cells grown aerobically and exposed to other NO donors and hydrogen peroxide [61, 62].

This gene encodes for a 24 kDa monomeric protein containing two iron atoms, which form a non-heme diiron center, as assessed by UV-visible and electron paramagnetic resonance (EPR) spectroscopies [63, 64]. This protein has the typical four-helix bundle fold of diiron proteins, as predicted by homology-based modelling and later confirmed by X-ray crystallography (Figure I.10) [65, 66].

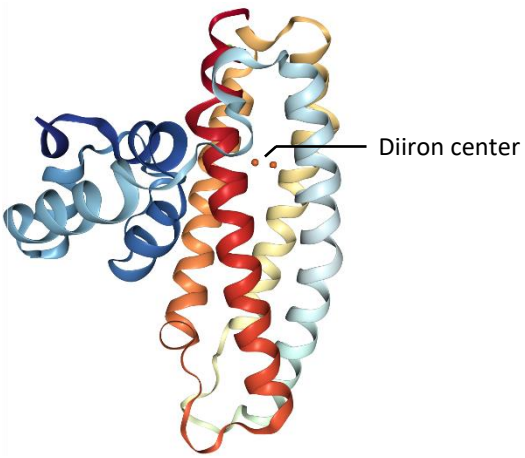

Figure I.10. Crystal structure of the *E. coli* RIC protein (PDB ID: 5FNN), at 2.09 Å resolution. The structure of the staphylococcal homologue has not been determined yet.

It was found that *ytfE* knock-out mutants of *E. coli* suffer growth impairment under nitrosative and oxidative stress, both under aerobic and anaerobic conditions [60, 63]. These mutants also exhibited diminished activity of important enzymes containing iron-sulfur (Fe-S) clusters, such as aconitase and fumarase, which was correlated to nitrosative and oxidative damage to the clusters [63, 67]. Moreover, contrary to the wild type strain, the mutants were not able to recover these activities once the stress was removed: full catalytic recovery was only achieved upon addition of the purified *ytfE* gene product [67].

Fe-S clusters are ubiquitous prosthetic groups that are involved in a myriad of cellular processes, fulfilling redox, catalytic and regulatory functions. These clusters are one of the major targets of ROS and RNS: reaction with NO forms stable dinitrosyl-iron complexes, whereas reaction with other RNS and ROS produces oxidized and unstable forms of the clusters [64, 67]. Both stresses render the Fe-S clusters catalytically inactive and their repair requires reinsertion of iron [64, 67].

As mentioned earlier, the *ytfE* gene product of *E. coli* was shown to be necessary to restore the activity of oxidatively and nitrosatively-damaged Fe-S enzymes. Additionally, it was also demonstrated that it is able to donate iron to apo-forms of Fe-S proteins [61].

Analysis of amino acid sequence databases revealed that homologues of the *ytfE* gene product occur in Gram-positive and Gram-negative bacteria, protozoa and fungi, including several human

pathogens [58, 64]. Alignment of their amino acid sequences showed a set of highly conserved residues, which were proposed to constitute the ligand sphere for the diiron center [64, 68]. Moreover, the predicted secondary structures of these proteins are also consistent with a four-helix bundle fold [64]. Since this was the first diiron protein for which a role in the repair of Fe-S clusters was observed, the name Repair of Iron Centers (RIC) was proposed for this new family of proteins [68].

The expression of the *scdA* gene of *S. aureus* is also induced by oxidative and nitrosative stress conditions, and encodes a RIC protein that shares 25% identity and 46% similarity of amino acid sequence with the RIC of *E. coli* [67]. The RIC proteins of *S. aureus* and *E. coli* were demonstrated to have similar biochemical roles, since the *S. aureus* RIC was able to suppress the enhanced sensitivity to oxidative stress of an *E. coli* knock-out mutant of *ric* [68].

Similar to what was previously described for *E. coli*, lower activities of the Fe-S enzymes aconitase and fumarase were demonstrated for *ric* knock-out mutants of *S. aureus*, which were only restored after addition of recombinant RIC [68]. Recently, RIC was proved to contribute to the virulence of *S. aureus* and to offer protection against oxidative stress [69]. It was observed that the survival of *ric* knock-out mutants was lower when exposed to hydrogen peroxide and within macrophages. Notably, the viability of these mutants was still lower in macrophages inhibited of producing NO, but similar to the wild-type strain in macrophages inhibited of producing ROS, thus highlighting the protective role of RIC in oxidative conditions. The viability was restored by in *trans* complementation. Studies were also performed in the infection model *Galleria* (*G.*) *mellonella*, a wax moth that only has innate immunity. Survival of *G. mellonella* infected with the *ric* knock-out mutant was approximately 2.5-times higher. The expression of *ric* was also demonstrated to increase over the course of the infection, reaching an approximate 20-fold increase after 8 hours.

I.6. Aims of the study

Staphylococcus epidermidis and *Staphylococcus aureus* are important human pathogens and are extensively associated with biofilm-related infections on implanted medical devices, which are very difficult to treat due to the biofilm resistance to the host immune system and antibiotics. Moreover, these pathogens pose serious health and economic burdens worldwide.

Since the pathogenic potential of *S. epidermidis* was not recognized for a long time, there is a lack of knowledge regarding its pathogenicity and defense mechanisms against the host immune system. Although *S. epidermidis* is related to *S. aureus*, these species differ significantly and, therefore, knowledge already obtained for *S. aureus* cannot be directly extrapolated to *S. epidermidis*. On the

other hand, while the resistance of *S. aureus* has been studied in its planktonic state, the defense mechanisms of this pathogen while in the biofilm state remain to be fully elucidated.

Therefore, it is pivotal to understand how *S. epidermidis* and *S. aureus* cope with the immune mechanisms of the host, namely the oxidative and nitrosative stress imposed by immune effectors, to enable the development of new antimicrobial strategies. For this purpose, the work aimed to:

- Analyze the expression levels of *S. epidermidis* genes whose products share significant amino acid sequence similarity to proteins known to contribute to NO protection, namely *hmp* and *ric*, under nitrosative stress conditions;
- Construct *S. epidermidis* knock-out strains of *hmp* and *ric;*
- Study the growth behavior, *in vitro* viability and ability to produce biofilm of the *S. epidermidis* mutants, under oxidative and nitrosative stress conditions.
- Study the effect of nitrosative stress on the biofilm formation ability of *S. aureus* knock-out mutants of *hmp* and *ric.*

II. Materials and Methods

II.1. Bacterial strains, culture media and growth conditions

The bacterial strains used throughout this work are listed in Table II.1. For the sake of clarity, hereafter, the strain *S. aureus* USA300 JE2 will only be referred to as *S. aureus* JE2, and the strains *S. aureus* USA300 JE2 NE1744 and *S. aureus* USA300 JE2 NE1857 will only be referred to as *S. aureus* JE2 *hmp*::Tn and *S. aureus* JE2 *ric*::Tn, respectively. The presence of the transposon mutations of these strains was confirmed by PCR as described in Appendix VI.9.

Table II.1. Bacterial strains used in this work.

Strain	Features	Source
S. epidermidis		
RP62A	MRSE clinical isolate	F. Götz, University of Tübingen, Germany
1457	MSSE clinical isolate	H. Rohde, University of Hamburg, Germany
S. aureus		
RN4220	Restriction-defective derivative of NCTC8325	Laboratory stock
USA300 JE2	Plasmid-cured derivative of the CA-MRSA USA300 LAC	NARSA
USA300 JE2 NE1744	*hmp* transposon mutant of USA300 JE2	NARSA
USA300 JE2 NE1857	*ric* transposon mutant of USA300 JE2	NARSA
E. coli		
XL1-Blue	Host strain for routine cloning	Laboratory stock
DC10B	Δ*dcm* derivative of *E. coli* K12 DH10B	T. Foster, Trinity College Dublin, Ireland

MRSE: methicillin-resistant *S. epidermidis*
MSSE: methicillin-sensitive *S. epidermidis*
CA-MRSA: community-acquired methicillin-resistant *S. aureus*
NARSA: network on antimicrobial resistance in *S. aureus*
dcm: DNA cytosine methyltransferase

The composition of the culture media used throughout this work is detailed in Appendix VI.1. *Staphylococcus* were routinely cultured in TSB or BHI, whereas *E. coli* was routinely cultured in LB. When required, the culture media were supplemented with erythromycin at 10 μg mL^{-1}, for *E. coli* and

Staphylococcus, and chloramphenicol 15 μg mL^{-1} for *E. coli* or 10 μg mL^{-1} for *Staphylococcus*. Unless stated otherwise, all strains were grown under aerobic conditions, at 37 ^{O}C and 150 rpm. Stock cultures were prepared from overnight cultures and stored in 25% (v/v) glycerol, at – 80 ^{O}C. When needed, the stocks were thawed on ice and inoculated at 1% in culture medium.

II.1.1. Growth conditions for oxidative and nitrosative stress on planktonic cells

Overnight cultures of *S. epidermidis* RP62A, grown in TSB, were diluted in TSB supplemented with 0.5% (w/v) glucose (TSB-Glc) to an OD_{600} of 0.1. These cultures were grown at 37 ^{O}C and 150 rpm, either under aerobic conditions, in 100 mL Erlenmeyer flasks filled up to 20% of their total volume, or under microaerobic conditions, in 50 mL rubber stopper flasks filled up to 60% of their total volume. At an OD_{600} of 0.4, stress was induced by addition of spermine-NONOate to the final concentration of 200 μM, GSNO to the final concentrations of 50, 200 and 800 μM, and H_2O_2 to the final concentrations of 5, 10 and 20 mM. The cultures were grown at 37 ^{O}C and 150 rpm until the stationary phase was reached (approximately 8 hours). In total, three biological replicates were performed.

After 20 minutes of stress, induced as described above, aliquots of 100 μL were collected from each culture. These cell aliquots were serially diluted in PBS (10 mM Na_2HPO_4, 1.8 mM KH_2PO_4, 137 mM NaCl, 2.7 mM KCl, pH 7.4), from 10^{-1} to 10^{-5}-fold, and 5 μL of the dilutions 10^{-4} and 10^{-5} were plated on TSA, in duplicate. The plates were incubated at 37 ^{O}C overnight. Percentage of survival was calculated by determination of colony-forming units (CFUs), using Equation II.1, relative to the untreated culture.

$$\text{CFUs mL}^{-1} = \frac{\text{Number of colonies}}{\text{Volume plated in mL}} \times \text{dilution factor} \qquad \textbf{Equation II.1}$$

II.1.2. Growth conditions for oxidative and nitrosative stress on biofilms

The biofilm assays were initiated by dilution of overnight cultures in TSB-Glc, to an OD_{600} of 0.05. Overnight cultures of *S. epidermidis* RP62A, *S. epidermidis* 1457 and *S. aureus* JE2 were grown in TSB, while *S. aureus* JE2 *hmp*::Tn and *S. aureus* JE2 *ric*::Tn were grown in TSB supplemented with erythromycin at 10 μg mL^{-1}. The assays were performed in sterile, 96-well polystyrene flat-bottomed tissue-culture plates (Sarstedt). The wells were filled with 200 μL of diluted culture, and five replicates were prepared for each concentration tested. In total, three biological replicates were performed. All the conditions used are listed in Table II.2 and described below.

Condition 1 - 8 hours of stress, since inoculation: after plate inoculation, the stress was immediately applied by addition of GSNO or H_2O_2. Cells were statically incubated at 37 ^{O}C for 8 hours. At the end, biofilm quantification was performed as described in section II.2.

Condition 2 - 24 hours of stress since inoculation: the procedure was done similarly to that described for condition 1, but the cells were incubated for 24 hours.

Condition 3 - 1 hour of stress on a 4 hours old biofilm, followed by 3 hours of recovery: after plate inoculation, cells were statically incubated at 37 ^{O}C 4 hours. The planktonic culture was removed, the biofilms were washed twice with 200 µL of PBS and 200 µL of fresh TSB-Glc were added. Stress was applied for 1 hour by addition of GSNO or H_2O_2. After stress, the planktonic culture was removed and the biofilms were washed two times with 200 µL of PBS. To allow cells to recover, 200 µL of fresh TSB-Glc were added and the cells were statically incubated at 37 ^{O}C for 3 hours. At the end, biofilm quantification was performed as described in section II.2.

Condition 4 - 1 hour of stress on a 4 hours old biofilm, followed by 12 hours of recovery: the procedure was done similarly to that described for condition 3 but the cells were allowed to recover for 12 hours in the fresh medium.

Table II.2. Conditions tested for nitrosative and oxidative stresses on biofilms.

Condition	Stress	Concentrations Tested (mM)	Strains Tested
8h of stress since inoculation	GSNO	0.2	*S. aureus* JE2 *S. aureus* JE2 *hmp*::Tn *S. aureus* JE2 *ric*::Tn
	GSNO	0.05, 0.1, 0.2, 0.4, 0.8 and 1.0	*S. epidermidis* RP62A *S. epidermidis* 1457
	H_2O_2	2, 5, 10, 20 and 40	*S. epidermidis* RP62A *S. epidermidis* 1457
24h of stress since inoculation	GSNO	0.2 and 0.5	*S. aureus* JE2 *S. aureus* JE2 *hmp*::Tn *S. aureus* JE2 *ric*::Tn
1h of stress, on a 4h old biofilm followed by 3h of recovery	GSNO	0.2	*S. aureus* JE2 *S. aureus* JE2 *hmp*::Tn *S. aureus* JE2 *ric*::Tn
	GSNO	0.05, 0.1, 0.2, 0.4, 0.8 and 1.0	*S. epidermidis* RP62A *S. epidermidis* 1457
	H_2O_2	2, 5, 10, 20 and 40	*S. epidermidis* RP62A *S. epidermidis* 1457
1h of stress, on a 4h old biofilm followed by 12h of recovery	GSNO	0.05, 0.1, 0.2, 0.4, 0.8 and 1.0	*S. epidermidis* RP62A
	H_2O_2	2, 5, 10, 20 and 40	*S. epidermidis* RP62A

II.2. Quantification of biofilm biomass

The semiquantitative microtiter plate assay described by Gordon Christensen [70] was followed with some modifications. At the end of the bacterial growths described in section II.1.2, the planktonic cell culture was gently aspirated, to avoid disturbing the biofilm formed at the bottom of the well. The wells were washed two times with 200 µL of PBS, and the plate was incubated at 60 ^{O}C for 1 hour [71], to allow the biofilm to dry. After cooling the plate to room temperature, the biofilm was stained with 200 µL of 1% (v/v) crystal violet, for 20 minutes. The excess dye was rinsed off three times with 200 µL of PBS. The cellular biofilm was left to dry for approximately 20 minutes, by inverting the plate on absorbent paper. The dye was eluted by incubation with 200 µL of 33% (v/v) acetic acid for 10 minutes. The eluted dye was transferred to a clean plate and the absorbance was read at 570 nm with a microplate spectrophotometer (Multiskan™ GO Microplate Spectrophotometer, Thermo Scientific).

II.3. Extraction of total RNA and real-time quantitative reverse transcription polymerase chain reaction (qRT-PCR) assays

To assess the effect of nitrosative stress on the expression levels of *S. epidermidis* RP62A genes *hmp* and *ric*, total RNA extraction qRT-PCR assays were performed, as described below. All the commercial kits used are detailed in Appendix VI.3. In total, three independent RNA extractions were performed, which were analyzed in three independent qRT-PCR assays, in duplicate.

Overnight cultures of *S. epidermidis* RP62A, grown in LB, were diluted in fresh LB to an OD_{600} of 0.1. The cultures were incubated at 37 ^{O}C and 150 rpm, in both aerobic and microaerobic conditions (detailed in section II.1.1), and at an OD_{600} of 0.4 spermine-NONOate was added to a final concentration of 200 µM.

After 20 minutes of stress, cell aliquots were collected, to which a stop solution (5% concentrated phenol and 95% concentrated ethanol) was added. These aliquots were pelleted at 2 000 *x*g, for 5 minutes and flash-frozen in liquid nitrogen. Frozen pellets were kept at – 80 ^{O}C.

Total RNA extraction was achieved using the High Pure RNA Isolation Kit (Roche). Briefly, cell pellets were thawed on ice and resuspended in 200 µL of 10 mM Tris-HCl pH 8.0. Cells were lysed by incubation with lysozyme 2 mg mL^{-1} and lysostaphin 0.1 mg mL^{-1} at 37 ^{O}C for 30 minutes, followed by addition of 400 µL of Lysis/Binding Buffer and vortexing. The lysates were transferred to a High Pure Filter Tube and the manufacturer's protocol was followed. Contaminating DNA was removed by using

Turbo DNA-*free* ™ Kit (Ambion), following the manufacturer's instructions. The absence of chromosomal DNA was confirmed by PCR, using oligonucleotides for the *S. epidermidis* housekeeping gene *gyrB* (see Appendix VI.2). RNA concentration and purity were evaluated in a Nanodrop ND-1000 UV-visible spectrophotometer (Thermo Fisher Scientifiic), and by agarose gel electrophoresis (see Appendix VI.6).

To synthesize complementary DNA (cDNA), 3 µg of the total RNA extracted were reverse transcribed using the Transcriptor High Fidelity cDNA Synthesis Kit (Roche).

The qRT-PCR assays were conducted in a LightCycler ® 480 (Roche), using ~3 µg of cDNA, 0.5 µM of gene-specific oligonucleotides (see Appendix VI.2), PCR-grade H_2O and the LightCycler® 480 SYBR Green Maxter Mix (Roche), which contains FastStart Taq DNA polymerase, reaction buffer, dNTP mix, SYBR Green I dye and $MgCl_2$. The qRT-PCR program used can be found in Appendix VI.5.

The expression levels of *S. epidermidis hmp* and *ric* genes were normalized relative to the housekeeping gene *gyrB*, which is commonly used in these studies [72]. The fold change in gene expression, after 20 minutes of stress with 200 µM spermine-NONOate, induced as described in section II.1.2, was calculated according to the comparative threshold (C_T) method (Equation II.2) [73].

$$\text{Fold Change in Gene Expression} = \frac{2^{[\,(\text{CT untreated sample}) - (\text{CT stressed sample})\,]\ \text{target gene}}}{2^{[\,(\text{CT untreated sample}) - (\text{CT stresses sample})\,]\ gyrB}} \qquad \textbf{Equation II.2}$$

II.4. Construction of *S. epidermidis hmp* and *ric* deletion strains

To construct *S. epidermidis hmp* and *ric* deletion mutants, the allelic replacement mutagenesis protocol described by Ian Monk and colleagues was followed [74]. All oligonucleotides used, and the respective sequences, are listed in Appendix VI.2.

The scheme followed to prepare the recombinant plasmids for allelic replacement is outlined in Figure II.1. Briefly, the upstream and downstream regions flanking the genes to be deleted were PCR-amplified from genomic DNA (gDNA) of *S. epidermidis* RP62A (extracted as described in Appendix VI.8.2) using the following pairs of oligonucleotides (see Table VI.2): ric_A/ric_B and ric_C/ric_D to amplify flanking regions of ~500 bp of *ric*, hmp_A/hmp_B and hmp_C/hmp_D to amplify flanking regions of ~500 bp of *hmp*, and hmp_A2/hmp_B and hmp_C/hmp_D2 to amplify flanking regions of ~800 bp of *hmp*.

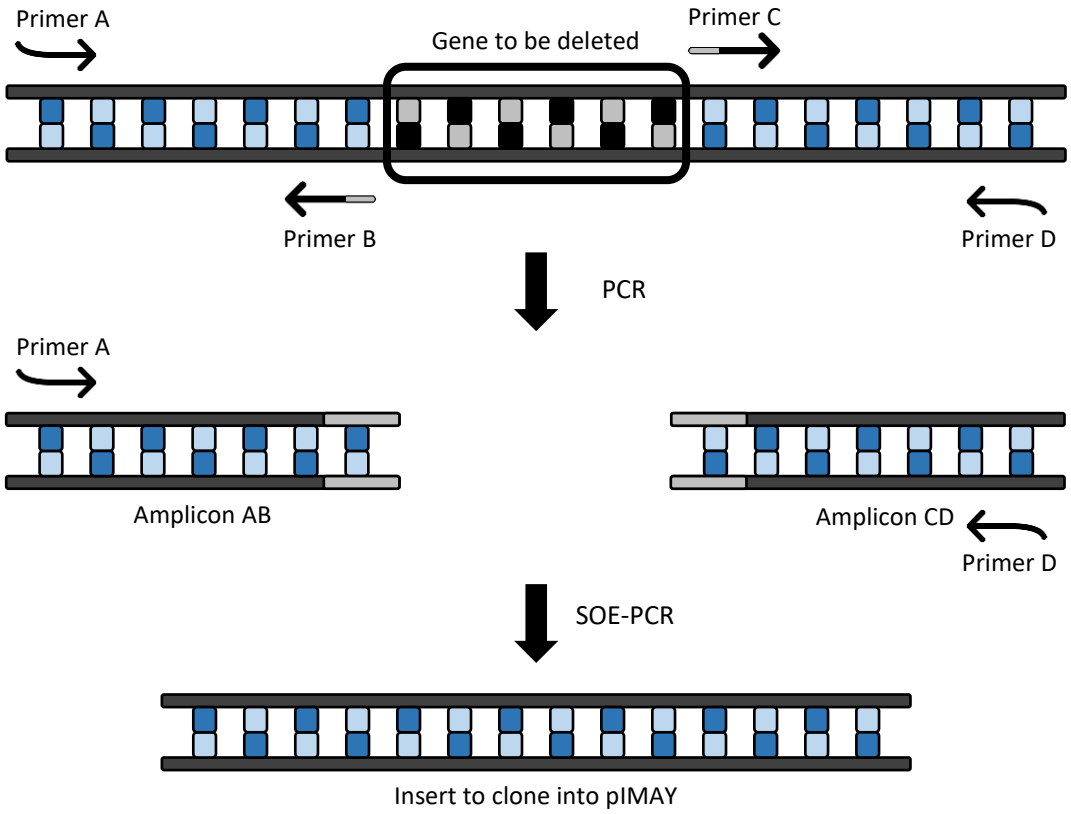

Figure II.1. Scheme of the construction of the DNA inserts for the generation of *S. epidermidis hmp* and *ric* deletions, by allelic replacement, using pIMAY. The highlighted parts of primers B and C, and of the amplicons AB and CD, represent the complementary regions for SOE-PCR.

The oligonucleotides B and C were designed so that the 3' region of oligonucleotide B was complementary to the 5' region of oligonucleotide C, whereas the oligonucleotides A and D were designed to include restriction sites. The amplicons AB and CD thus produced were combined together through a splicing by overlap extension polymerase chain reaction (SOE-PCR), using the pair of oligonucleotides A and D. The resulting ABCD amplicons were digested with EcoRI and SalI in the case of *hmp*, and SacI and EcoRI in the case of *ric*, as described in Appendix VI.4. These fragments were ligated to the plasmid pIMAY (see Appendices VI.2 and VI.4), linearized with the same restriction endonucleases, originating the recombinant plasmids pIMAY-*ric*500 (flanking regions of ≈ 500 bp), pIMAY-*hmp*500 (flanking regions of ≈ 500 bp), pIMAY-*hmp*800 (flanking regions of ≈ 800 bp).

The recombinant plasmids were transformed into *E. coli* CD10B competent cells, which were prepared and transformed as described in Appendix VI.7.1. These plasmids were isolated from *E. coli* as described in Appendix VI.8.1 and the insert sequence was confirmed by Sanger sequencing (STAB VIDA).

After confirmation of the inserts sequence, the recombinant plasmids isolated from *E. coli* DC10B were transformed into *S. epidermidis* electrocompetent cells (see Appendix VI.7.3). The resulting colonies were screened by colony PCR (see Appendix VI.5), using the MCS oligonucleotides

of pIMAY (see Appendix VI.2). The positive clones were inoculated into BHI supplemented with chloramphenicol at 10 μg mL^{-1}, and incubated at 37 ^{O}C (non-permissive temperature of pIMAY) and 150 rpm, overnight, to induce recombination into the *S. epidermidis* chromosome. The complete protocol is described in Appendix VI.10.

II.5. Statistical Analysis

Statistical analyses were performed using GraphPad Prism (GraphPad software version 5.01, California, USA). Results were compared using two tailed unpaired Student's *t*-tests with a confidence interval of 95%.

III. Results

III.1. Behavior of *Staphylococcus* under oxidative and nitrosative stress

When faced with pathogens, the host immune system is triggered to fight-off the threat. The innate immune system is the first to respond and phagocytes, such as neutrophils and macrophages, are professional effectors of this response. Phagocytes eliminate microbes through phagocytosis: microbes are internalized into phagosomes, which maturate intro phagolysosomes with a highly acidic and hydrolytic lumen. Killing of phagocytosed microbes occurs through several mechanisms, mainly involving ROS and RNS [31].

Nonetheless, pathogens have evolved defense strategies against these responses. Whereas *S. aureus* has been described to be highly resistant to both oxidative and nitrosative stress [75, 76], the resistance of *S. epidermidis* has been less studied.

III.1.1. *S. epidermidis* RP62A

III.1.1.1 Planktonic cells exposed to stress

To evaluate the resistance of *S. epidermidis* to nitrosative and oxidative stress, cells grown in TSB supplemented with 0.5% (w/v) glucose (TSB-Glc), either aerobically or microaerobically, were treated with 200 µM of spermine-NONOate and various concentrations of GSNO and H_2O_2, at an OD_{600} of approximately 0.4 (Figure III.1).

Additionally, the survival of *S. epidermidis* after 20 minutes of stress was also inferred by determining the colony-forming units (CFUs) (Figure III.2). For this, cell aliquots were harvested, serially dilluted in PBS, and plated on TSA.

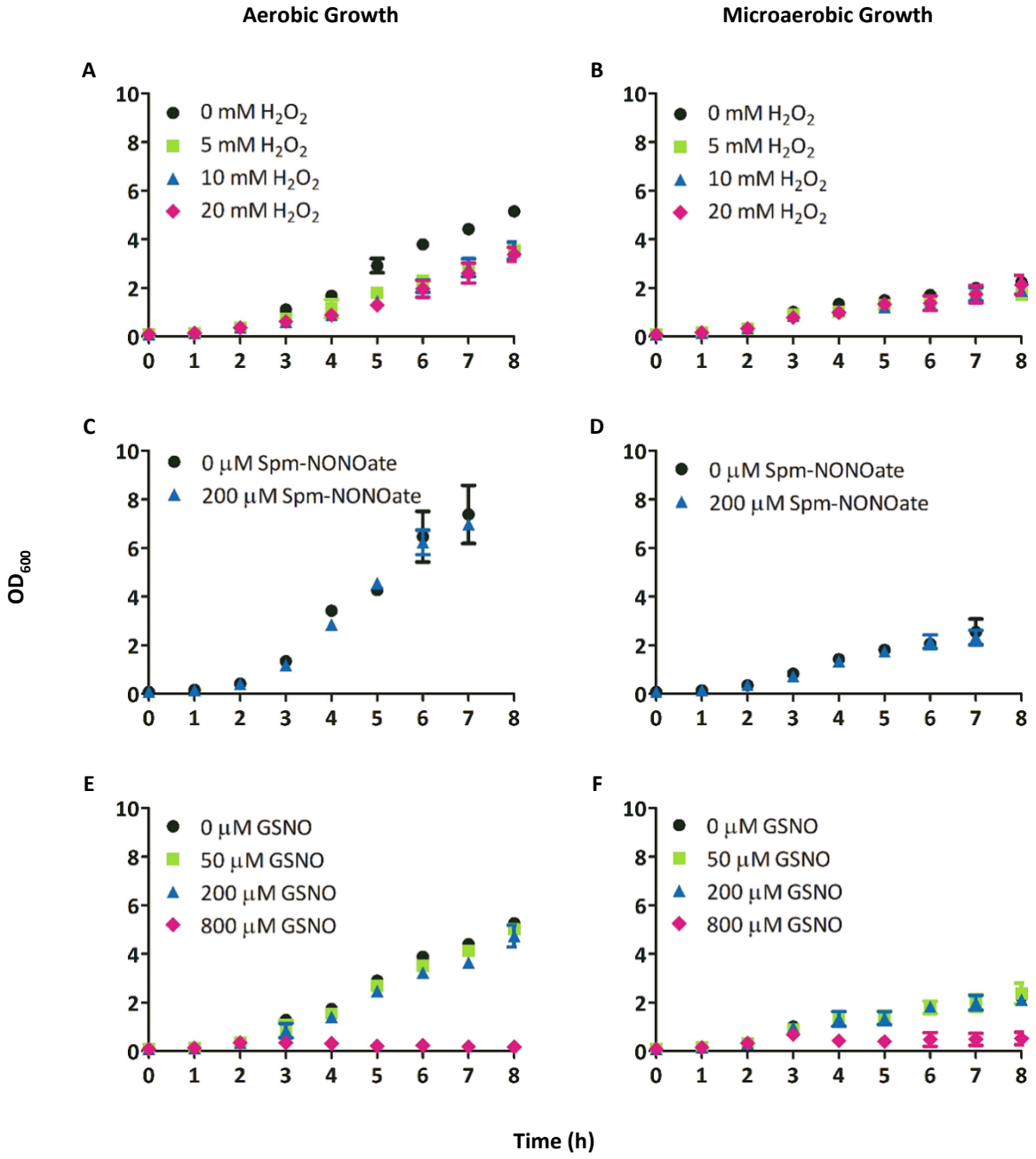

Figure III.1. Effect of nitrosative and oxidative stress on the growth of *S. epidermidis* RP62A. *S. epidermidis* cells were grown in TSB-Glc, under aerobic (A, C, E) or microaerobic (B, D, F) conditions, and treated with 5, 10 and 20 mM H_2O_2 (A, B), 200 µM spermine-NONOate (C, D), and 50, 200 and 800 µM GSNO (E, F), at an OD_{600} of approximately 0.4. Points represent the mean of at least three independent assays and bars the standard deviation. Spm, spermine.

S. epidermidis exhibited an oxygen-dependent growth behavior (Figure III.1). Under aerobic conditions (Figure III.1.A), concentrations up to 20 mM of H_2O_2 only exerted a slight but significant effect on the growth of *S. epidermidis*, whereas under microaerobic conditions (Figure III.1.B) no effect was observed. Under aerobic and microaerobic conditions (Figure III.1.C-F), concentrations up to 200 µM of spermine-NONOate and GSNO did not cause growth inhibition, whereas 800 µM GSNO induced

a severe growth arrestment. Moreover, for the same initial concentration of NO-donor (*i.e.*, 200 µM), spermine-NONOate and GSNO had a similar effect.

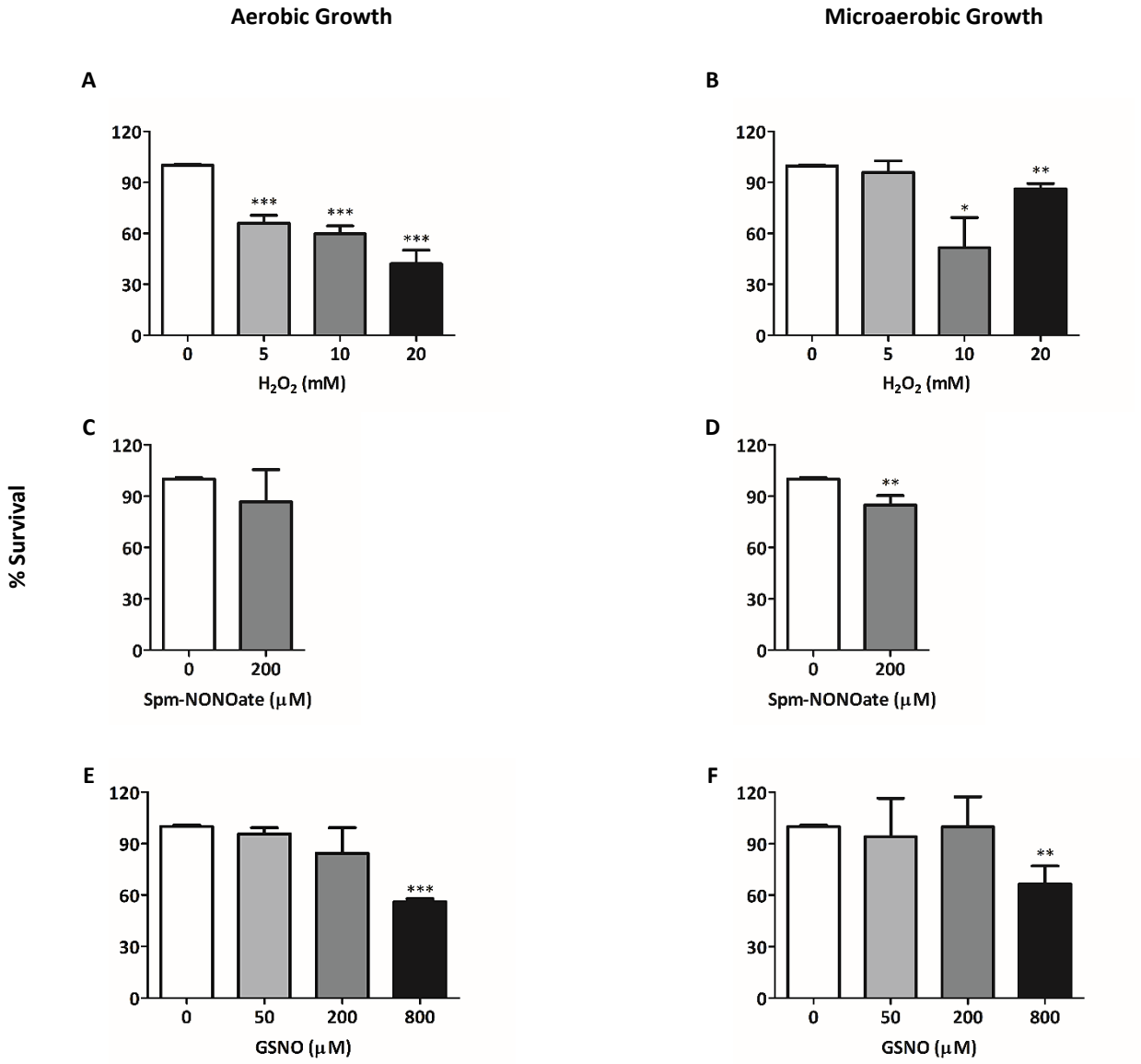

Figure III.2. Effect of nitrosative and oxidative stress on the survival of *S. epidermidis* RP62A. *S. epidermidis* RP62A cells were grown in TSB-Glc, under aerobic (A, C, E) or microaerobic (B, D, F) conditions, and treated with 5, 10 and 20 mM H_2O_2 (A, B), 200 µM of spermine-NONOate (C, D), and 50, 200 and 800 µM of GSNO (E, F), at an OD_{600} of approximately 0.4. After 20 minutes of stress, cells aliquots were serially diluted in PBS and plated on TSA, for determination of CFUs mL^{-1}. Percent survival values represent the ratio of CFUs mL^{-1} of treated to untreated culture. Error bars represent mean ± SD ($n \geq 2$). Asterisks represent statistically significant data, relative to the control; **P* < 0.05, ***P* < 0.01, and ****P* < 0.0001. Spm, spermine.

Oxidative stress induced with H_2O_2 exerted a greater effect on *S. epidermidis* survival under aerobic rather than microaerobic conditions (Figure III.2.A-B). Under aerobic conditions, *S. epidermidis* survival decreased with increasing concentrations of H_2O_2. A concentration of 20 mM H_2O_2 induced a

decrease in survival of ~58%, under aerobic conditions, but only of ~14% under microaerobic conditions.

The survival of *S. epidermidis* decreased only slightly (~15%) after 20 minutes of nitrosative stress induced with 200 µM of spermine-NONOate, under aerobic and microaerobic conditions (Figure III.2.C-D). Concentrations of GSNO up to 200 µM did not significantly affect the survival of *S. epidermidis* (Figure III.2.E-F). Notably, under microaerobic conditions, while 200 µM of spermine-NONOate reduced the survival of *S. epidermidis* by ~15%, 200 µM of GSNO did not affect survival. A significant decrease in survival was only observed with 800 µM GSNO: ~44% and ~33% under aerobic and microaerobic conditions, respectively.

III.1.1.2. Expression levels of flavohemoglobin (*hmp*) and repair of iron centers (*ric*) under nitrosative stress

The *hmp* and *ric* genes of *S. epidermidis* encode for flavohemoglobin and RIC proteins, respectively. These proteins share significant amino acid sequence identity and similarity to the flavohemoglobin and RIC of *E. coli*, which are known to protect against nitrosative stress [56, 64].

To assess the effect of nitrosative stress on the expression levels of these genes, cells of *S. epidermidis* grown in LB either aerobically or microaerobically, until the early-exponential phase (OD_{600} ~ 0.4), were subjected to a 20 minutes stress with 200 µM of spermine-NONOate (NO donor). Total RNA was extracted from these cells, purified and reverse transcribed to cDNA, which served as template for qRT-PCR. The quantification of the expression levels of *hmp* and *ric* were normalized relative to the housekeeping gene *gyrB*, which is typically used in these studies [72], and the fold change relative to untreated cells is presented in Figure III.3.

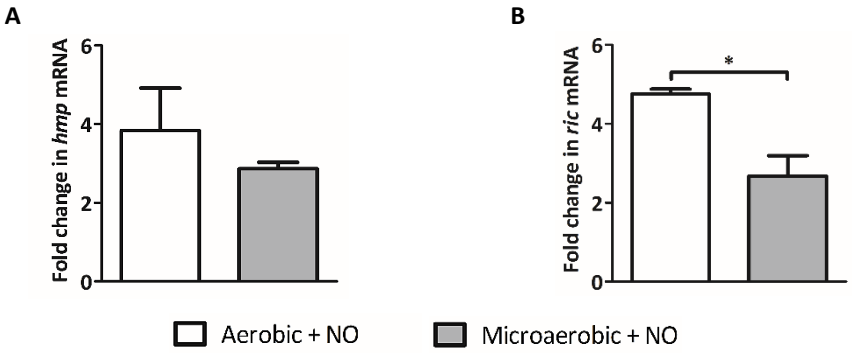

Figure III.3. Effect of nitrosative stress on the transcription levels of *S. epidermidis* RP62A *hmp* and *ric* genes. The fold change of the expression levels of *hmp* (A) and *ric* (B), under aerobic (white bars) and microaerobic (gray bars) conditions, upon exposure to 200 µM spermine-NONOate for 20 minutes, is indicated. Fold change values represent the ratio of the expression levels of treated to untreated culture, normalized relative to *gyrB*. Error bars represent mean ± SD ($n \geq 2$). Asterisks represent statistically significant data; $*P < 0.05$.

The expression levels of the *S. epidermidis* genes *hmp* and *ric*, in response to the nitrosative stress imposed by 200 µM spermine-NONOate, were affected similarly and dependent on the oxygen conditions (Figure III.3). Under aerobic conditions, *hmp* and *ric* were upregulated ~5-fold, whereas under microaerobic conditions they were only upregulated ~3-fold.

III.1.1.3. Biofilms exposed to stress

Biofilm production is one of the most important virulence factors of *S. epidermidis* and, accordingly, the infections caused by these bacteria are extensively associated with biofilm formation on indwelling or implanted medical devices [6]. In the biofilm state, cells exhibit higher resistance to several assaults, namely antibiotics and phagocytosis. Biofilm formation is a sequential process comprising cellular aggregation, accumulation, maturation and dispersal [7].

Despite the clinical significance of *S. epidermidis* biofilms, the effect of oxidative and nitrosative stress on their formation remains poorly understood. Hence, we have performed the study of *S. epidermidis* biofilms upon exposure to various concentrations of GSNO or H_2O_2. To analyze the different stages of the biofilm formation process, cells were exposed to the stress prior to biofilm formation or on already established biofilms. In the first case, biofilm quantification was performed 8 hours after stress. In the second case, stress was induced for 1 hour on 4-hour old biofilms, and biofilm quantification was performed either 3 or 12 hours after stress removal, to assess whether cells were able to recover over time.

In these conditions, for the untreated cells (Figure III.4), the amount of biofilm produced after 8 hours of continuous growth and after 8 hours of growth with exchange of culture media at the 5th and 6th hours (equivalent to a 4-hour old biofilm + 1 hour of stress + 3 hours of recovery) did not change significantly. However, when cells were cultured for 17 hours, the amount of biofilm formed was significantly lower (~25% decrease).

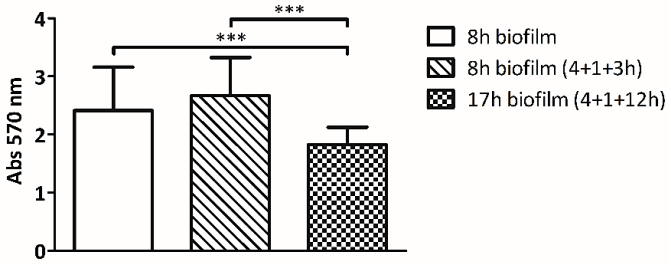

Figure III.4. Biofilm formation of *S. epidermidis* RP62A under normal growth conditions. *S. epidermidis* was grown in TSB-Glc for 8 hours (solid bar), for 8 hours with exchange of culture media at the 5th and 6th hours (striped bar), and for 17 hours with exchange of culture media at the 5th and 6th hours (plaid bar). Biofilms were quantified by staining with 1% (v/v) crystal violet and absorbance measurement at 570 nm. Error bars represent mean ± SD ($n \geq 30$). Asterisks represent statistically significant data; ***$P < 0.0001$.

Exposure of non-adherent cells to oxidative stress (Figure III.5.A), led to a decrease of biofilm formation of ~79% when 10 mM H_2O_2 were used. Higher concentrations abrogated biofilm formation (decrease of over ~97%). When oxidative stress was inflicted on established biofilms and the cells were allowed to recover for 3 hours (Figure III.5.C), concentrations of H_2O_2 up to 5 mM caused a decrease of biofilm formation of ~35%, while 20 and 40 mM H_2O_2 caused a decrease of ~77% and 91%, respectively. After 12 hours of recovery (Figure III.5.E), concentrations of H_2O_2 up to 5 mM caused a decrease of ~20%, while 10-40 mM H_2O_2 caused a decrease of ~36%.

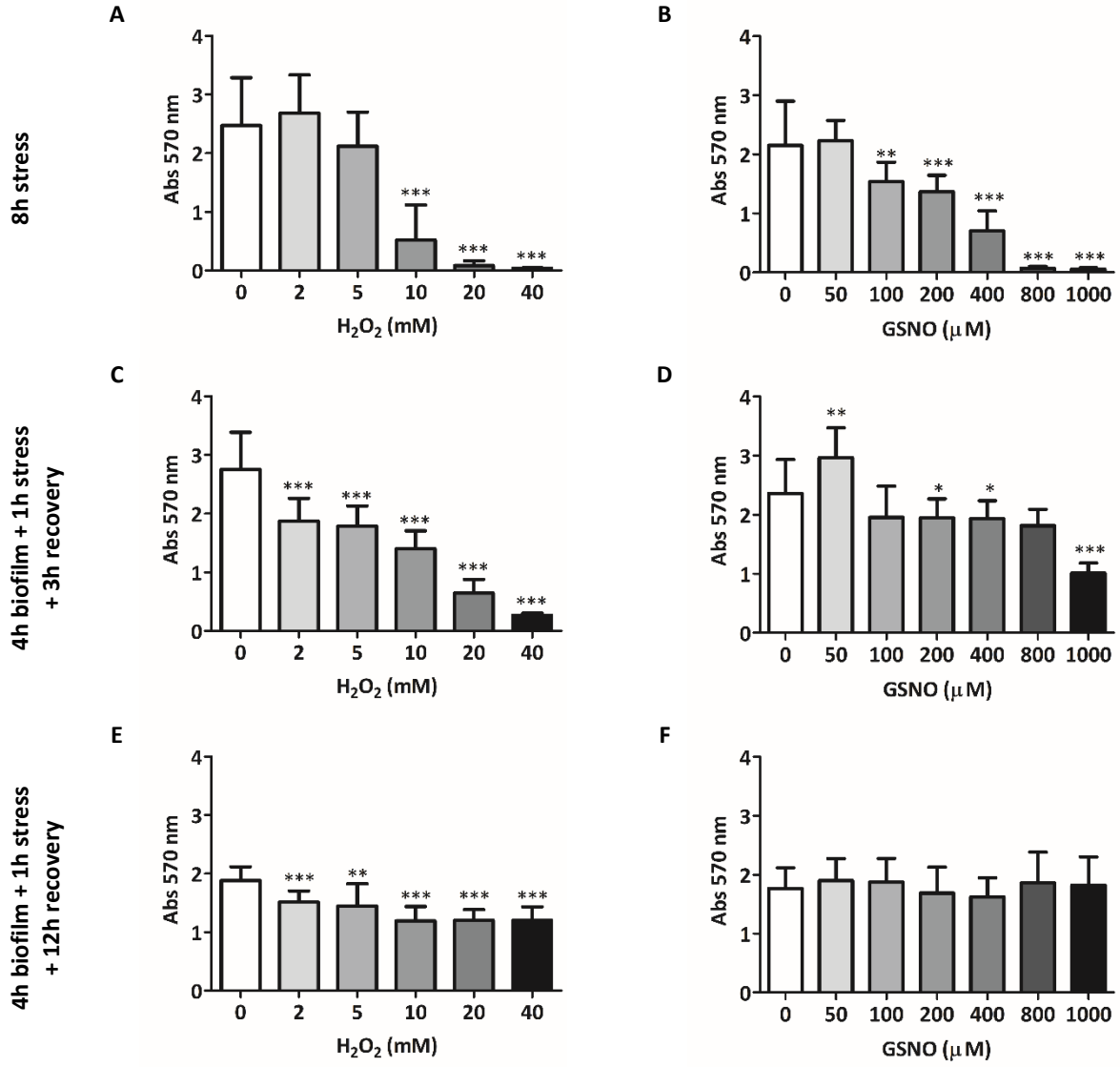

Figure III.5. Effect of nitrosative and oxidative stress on the biofilm formation of *S. epidermidis* RP62A. *S. epidermidis* was grown in TSB-Glc and treated with H_2O_2 (A, C, E) and GSNO (B, D, F). The stress was either added at inoculation time, and the biofilm quantified after 8 hours (A, B), or added to a 4-hour old biofilm, for 1 hour, and the biofilm quantified after 3 (C, D) or 12 hours (E, F) of recovery. Biofilms were quantified by staining with 1% (v/v) crystal violet and absorbance measurement at 570 nm. Error bars represent mean ± SD ($n \geq 10$). Asterisks represent statistically significant data, relative to untreated cells; $*P < 0.05$, $**P < 0.01$, and $***P <$

When cells were exposed to nitrosative stress before adherence (Figure III.5.B), the biomass of biofilm formed decreased with increasing concentrations of GSNO, reaching a maximum decrease of ~97% at 800 µM GSNO. Less prominent effects were observed when nitrosative stress was imposed for 1 hour on already established biofilms. After 3 hours of recovery (Figure III.5.D), GSNO concentrations up to 800 µM induced a decrease on biofilm formation of ~20%, whereas 1 000 µM GSNO induced a decrease of ~57%. After 12 hours of recovery (Figure III.5.F), no discernible differences were observed on the amount of biofilm produced.

Overall, the biofilm formation capacity of *S. epidermidis* RP62A was more affected when the stress was inflicted on cells not yet adherent, rather than on already established biofilms.

III.1.2. *S. epidermidis* 1457: biofilms exposed to stress

Biofilm formation varies among *S. epidermidis* strains, in particular among clinical isolates. For this reason, the effect of oxidative and nitrosative stress was also investigated on biofilms of another strain of *S. epidermidis*, namely 1457, which is a clinical isolate characterized by a strong biofilm production. These assays were performed similarly to those described for *S. epidermidis* RP62A.

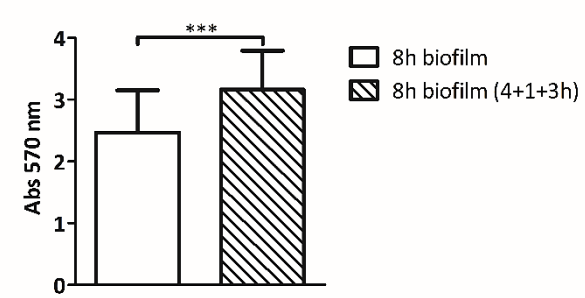

Figure III.6. Biofilm formation of *S. epidermidis* 1457 under normal growth conditions. *S. epidermidis* was grown in TSB-Glc for 8 hours (solid bar) and for 8 hours with exchange of culture media at the 5th and 6th hours (striped bar). Biofilms were quantified by staining with 1% (v/v) crystal violet and absorbance measurement at 570 nm. Error bars represent mean ± SD ($n \geq 24$). Asterisks represent statistically significant data; ***$P < 0.0001$.

For the untreated cells (Figure III.6), a significant increase (~28%) in the biomass of biofilm produced was observed when the cells were grown for 8 hours with exchange of culture media at the 5th and 6th hours (equivalent to a 4-hour old biofilm + 1 hour of stress + 3 hours of recovery), compared to when the culture media was not exchanged.

Treatment with H_2O_2 prior to biofilm establishment (Figure III.7.B) prompted a decrease in biofilm production which increased with increasing concentrations of stress. At 20 mM H_2O_2, a decrease of ~94% was observed. After 3 hours of recovery, biofilms subjected to oxidative stress (Figure III.7.D) exhibited a ~40% decrease in biofilm biomass for concentrations of H_2O_2 up to 10 mM. A decrease of ~81% was induced by 40 mM H_2O_2.

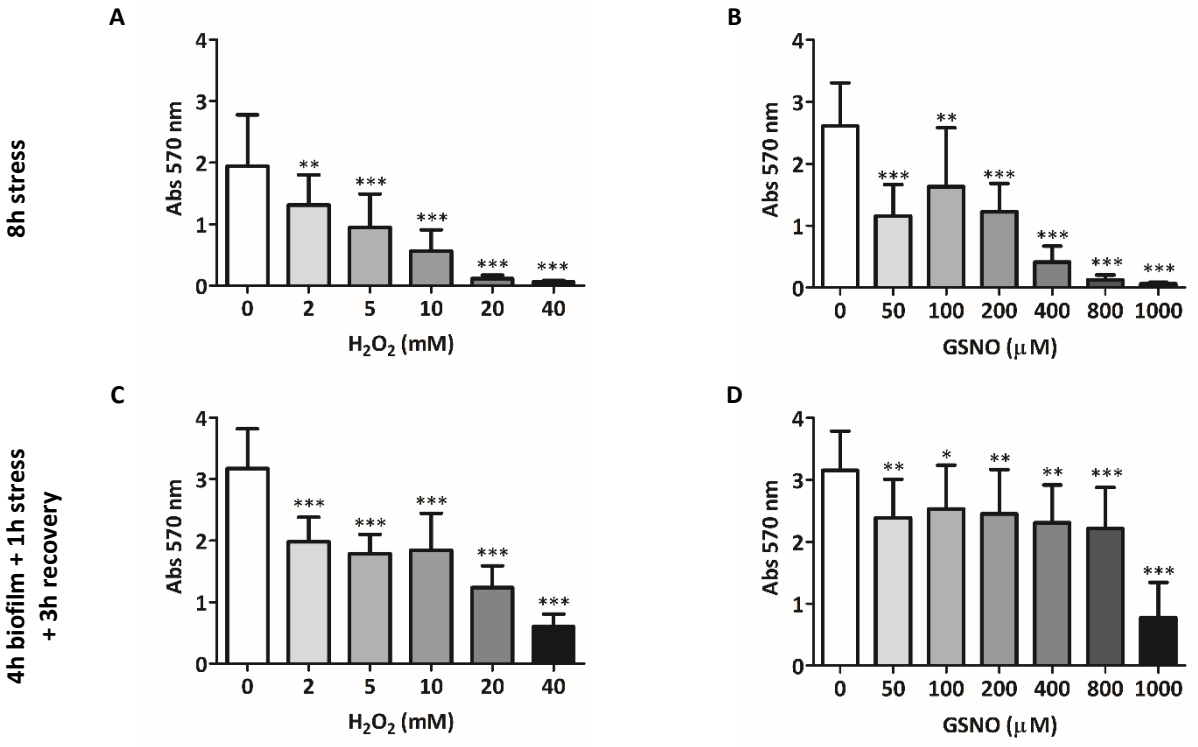

Figure III.7. Effect of nitrosative and oxidative stress on the biofilm formation of *S. epidermidis* 1457. *S. epidermidis* was grown in TSB-Glc and treated with H_2O_2 (A, C) and GSNO (B, D). The stress was either added at inoculation time, and the biofilm quantified after 8 hours (A, B), or added to a 4-hour old biofilm, for 1 hour, and the biofilm quantified after 3 hours of recovery (C, D). Biofilms were quantified by staining with 1% (v/v) crystal violet and absorbance measurement at 570 nm. Error bars represent mean ± SD (n ≥ 12). Asterisks represent statistically significant data, relative to untreated cells; **P* < 0.05, ***P* < 0.01, and ****P* < 0.0001.

Exposure to nitrosative stress before adherence (Figure III.7.A), caused a decrease of the amount of biofilm produced to approximately half, for 50 and 200 µM GSNO, whereas 800 and 1 000 µM GSNO strongly inhibited biofilm formation. GSNO concentrations up to 800 µM caused a ~20-29% decrease in biofilm biomass, when biofilms were exposed to 1 hour of nitrosative stress and allowed to recover for 3 hours (Figure III.7.C). A more prominent decrease, of ~75%, was observed for 1 00 µM.

More pronounced effects were observed when *S. epidermidis* 1457 was subjected to stress before adhesion, compared to those observed on established biofilms.

III.1.3. *S. aureus* JE2: biofilms exposed to stress

It has already been demonstrated that the bacterial proteins flavohemoglobin and RIC contribute to the protection of *S. aureus* against nitrosative stress [68, 77]. However, the protective role of these proteins has not been studied on *S. aureus* biofilms. To look into this question, *S. aureus hmp*

and *ric* transposon mutants were obtained from the Nebraska Transposon Mutant Library. The presence of the desired mutations was confirmed, by PCR (Appendix VI.7).

To study the effect of nitrosative stress on the biofilm formation of *S. aureus* JE2 *hmp*::Tn and *ric*::Tn, cells were grown in TSB-Glc and treated with GSNO. Biofilms assays were performed similarly to the ones performed for *S. epidermidis*. Cells were exposed to GSNO prior to biofilm formation or on already established biofilms (Figure III.8). In the first case, biofilm quantification was performed either 8 or 24 hours after stress. In the second case, stress was induced for 1 hour on 4-hour old biofilms, and biofilm quantification was performed 3 hours after stress removal.

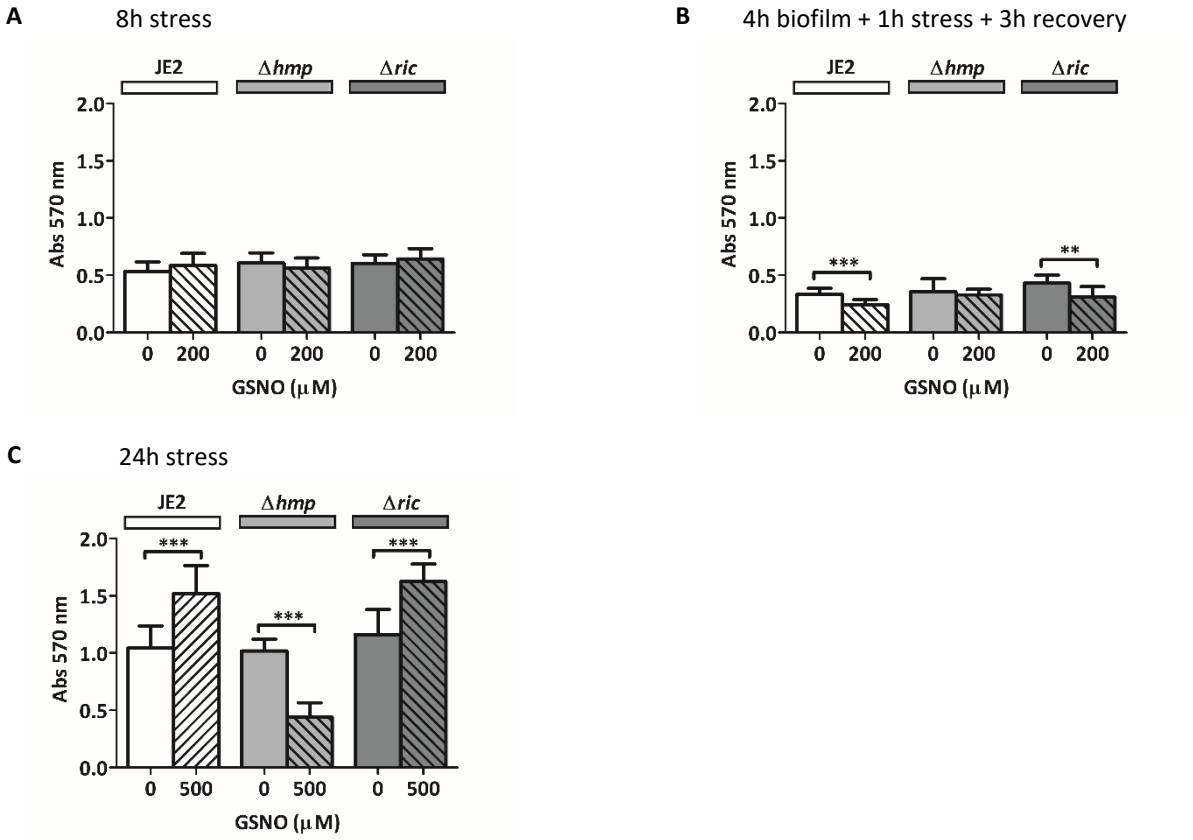

Figure III.8. Effect of nitrosative stress on the biofilm formation of *S. aureus* JE2 and the derived transposon mutants of *hmp* and *ric*. *S. aureus* JE2 and mutants were grown in TSB-Glc and treated with GSNO. (A) Stress was induced with 200 µM GSNO at inoculation time, and the biofilm was quantified after 8 hours. (B) Stress was induced with 200 µM GSNO on a 4-hour old biofilm, for 1 hour, and the biofilm was quantified after 3 hours of recovery. (C) Stress was induced with 500 µM GSNO at inoculation time, and the biofilm was quantified after 24 hours. Biofilms were quantified by staining with 1% (v/v) crystal violet and absorbance measurement at 570 nm. Error bars represent mean ± SD ($n \geq 9$). Asterisks represent statistically significant data; $^{**}P < 0.01$, and $^{***}P < 0.0001$.

When nitrosative stress was imposed for 1 hour on established biofilms and the cells were allowed to recover for 3 hours (Figure III.8.B), no significant difference in the amount of biofilm produced by the Δ*hmp* mutant was observed, while a decrease of ~27% was observed for the wild-type and Δ*ric* strains.

The effect observed for non-adhered cells exposed to nitrosative stress was dependent on the GSNO concentration and time of exposure. Stress induced with 200 µM GSNO for 8 hours (Figure III.8.A), did not cause discernible differences in the biomass of biofilm produced for the wild-type and mutant strains. However, when the stress was imposed for 24 hours with 500 µM GSNO (Figure III.8.C), an increase of biofilm biomass of ~40% was observed for the wild-type and Δ*ric* mutant strains, while a decrease of ~57% was observed for the Δ*hmp* mutant.

Established biofilms of *S. aureus* JE2 revealed a higher susceptibility to nitrosative stress than non-adhered cells.

III.2. Construction of *S. epidermidis* knock-out strains

Whilst the protective role of flavohemoglobin and RIC against oxidative and nitrosative stress has been described for *E. coli* and *S. aureus* [56, 64, 68, 77], it has not been explored in *S. epidermidis*. To this end, we sought to construct *S. epidermidis hmp* and *ric* knock-out mutants. An allelic replacement mutagenesis protocol for the creation of in-frame, unmarked deletion mutations in *S. epidermidis* has been described, and resorts to pIMAY, a low-copy, temperature-sensitive, shuttle (*E. coli*/staphylococcal) plasmid [78]. Therefore, three recombinant plasmids - pIMAY-*hmp*500, pIMAY-*hmp*800 and pIMAY-*ric*500 – were prepared by cloning the flanking regions of *hmp* and *ric* into pIMAY.

To construct the recombinant plasmids pIMAY-*hmp*500, pIMAY-*hmp*800 and pIMAY-*ric*500, the upstream and downstream flanking regions of *hmp* and *ric* were PCR-amplified from the genomic DNA of *S. epidermidis* RP62A (Figure III.9).

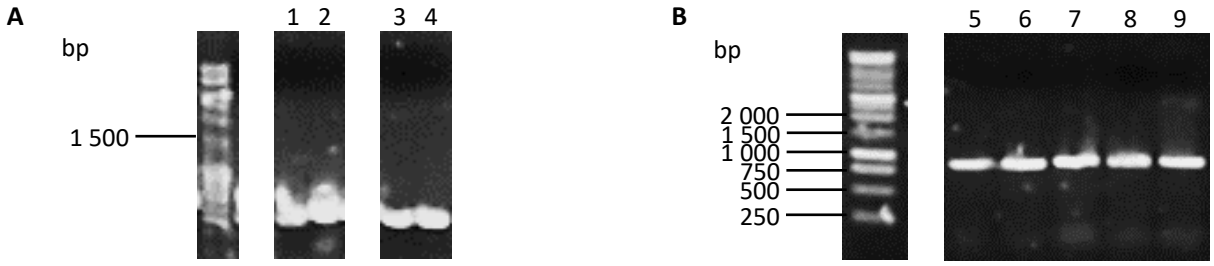

Figure III.9. Amplification of the flanking regions of the *hmp* and *ric* genes of *S. epidermidis* RP62A. (A) To construct pIMAY-*hmp*500, the upstream (1) and downstream (2) flanking regions of *hmp* were amplified from genomic DNA. The expected size of the amplicons is 584 and 633 bp, respectively. To construct pIMAY-*ric*500, the upstream (3) and downstream (4) flanking regions of *ric* were amplified from genomic DNA. The expected size of the amplicons is 584 and 577 bp, respectively. (B) To construct pIMAY-*hmp*800, the upstream (5-7) and downstream (8, 9) flanking regions of *hmp* were amplified from genomic DNA. The expected size of the amplicons is 885 and 908 bp, respectively. Electrophoresis was performed in 1% agarose gels, at 80 V.

These products were purified and joined together by SOE-PCR, as described in section II.7 (Figure III.10). Briefly, the oligonucleotides used to amplify each flanking sequence were designed so that the 3' end of the upstream flank would complement with the 5' end of the downstream flank. This overlapping complementary region served as a primer for a subsequent PCR reaction, which allowed the two flanks to be joined together using only oligonucleotides from the far ends of each flank.

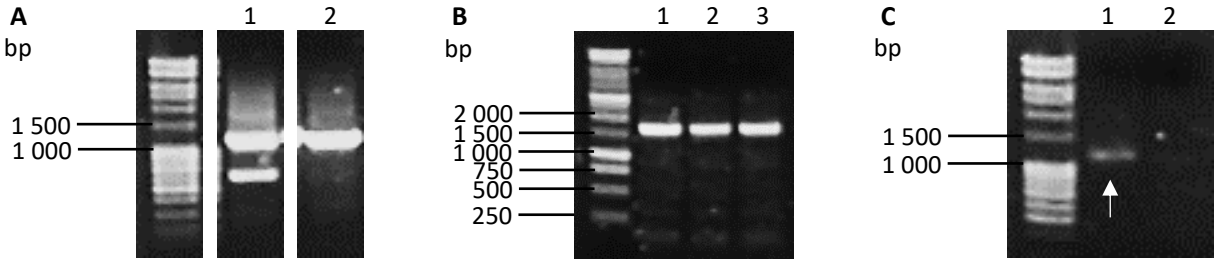

Figure III.10. Combination of the flanking regions of the *hmp* and *ric* genes of *S. epidermidis* RP62A. (A) To construct pIMAY-*hmp*500 and pIMAY-*ric*500, the upstream and downstream flanking regions of (1) *hmp* and (2) *ric* were fused by SOE-PCR. The expected size of the amplicons is 1 217 and 1 161 bp, respectively. (B) To construct pIMAY-*hmp*800, the upstream and downstream flanking regions of *hmp* were fused by SOE-PCR. The expected size of the amplicon is 1 793 bp. (C) SOE-PCR product for pIMAY-*hmp*500 (A-1), after gel extraction (see Appendix VI.8.3) and purification. Electrophoresis was performed in 1% agarose gels, at 80 V.

The purified SOE-PCR products were cloned into pIMAY, originating the recombinant plasmids pIMAY-*hmp*500, pIMAY-*hmp800* and pIMAY-*ric*500. These plasmids were subsequently transformed into *E. coli* DC10B (Figure III.11), and the insert sequence was confirmed by Sanger sequencing (STAB VIDA).

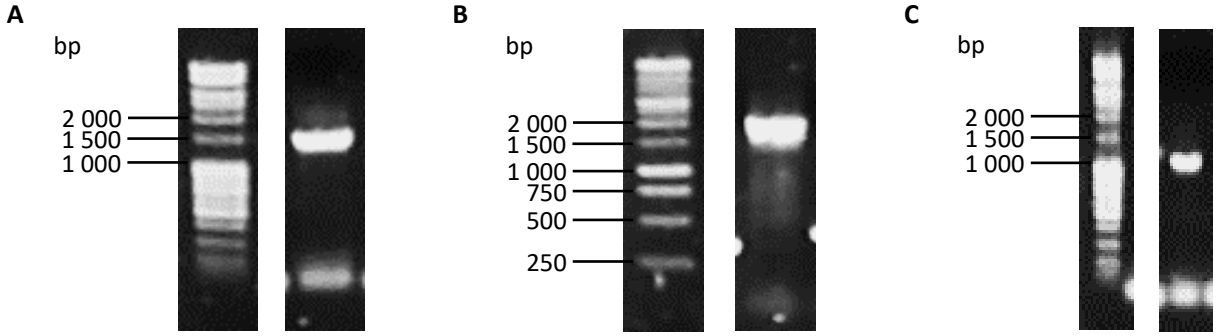

Figure III.11. Screening of *E. coli* DC10B transformed with the recombinant plasmids pIMAY-*hmp*500, pIMAY-*hmp*800 and pIMAY-*ric*500. To confirm the transformation of *E. coli* DC10B with (A) pIMAY-*hmp*500, (B) pIMAY-*hmp*800, and (C) pIMAY-*ric*500, colonies were screened by colony PCR, using the MCS_fwd and MCS_rev oligonucleotides of pIMAY. The expected size of the amplicons is 1 443, 2 025 and 1 329 bp, respectively. Electrophoresis was performed in 1% agarose gels, at 80 V.

To bypass the strong restriction barrier of *S. epidermidis*, which is mainly due to a type IV restriction enzyme that recognizes cytosine-methylated DNA [78], the recombinant plasmids were transformed into *E. coli* DC10B prior to electroporation into *S. epidermidis*. *E. coli* DC10B was derived

from the high-efficiency cloning strain DH10B, by deletion of *dcm*, which encodes for the DNA-cytosine methyltransferase.

After extraction from *E. coli* DC10B, the recombinant plasmids pIMAY-*hmp*500 and pIMAY-*ric*500 were electroporated into *S. epidermidis* RP62A. The presence of these plasmids in the resulting colonies was screened by colony PCR. Whereas two colonies were found to contain pIMAY-*hmp*500 (Figure III.12), none of the screened colonies were found to contain pIMAY-*ric*500 (34 colonies were screened).

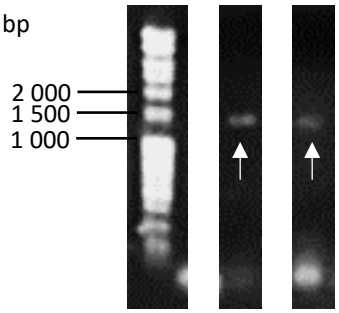

Figure III.12. Screening of *S. epidermidis* RP62A transformed with pIMAY-*hmp*500. After transformation, colonies were screened for the presence of the recombinant plasmid, by colony PCR, using the MCS_fwd and MCS_rev oligonucleotides of pIMAY. The expected size of the amplicon is 1 443 bp. Electrophoresis was performed in 1% agarose gels, at 80 V.

To promote the integration of pIMAY-*hmp*500 into the chromosome of *S. epidermidis* RP62A, the colonies that were confirmed to contain the recombinant plasmid were inoculated into BHI supplemented with chloramphenicol 10 µg mL^{-1}, and grown at 37 ^{O}C, overnight. However, no growth was observed. Therefore, ten additional experiments were tested over the course of two months, which included the following modifications:

- Lower concentrations of antibiotic: the colonies were inoculated into BHI supplement with 4, 6 or 8 µg mL^{-1} of chloramphenicol and grown at 37 ^{O}C, overnight. No growth was observed.

- Pre-culture at 28 ^{O}C: the colonies were first inoculated into BHI supplemented with chloramphenicol 10 µg mL^{-1}, and grown at 28 ^{O}C (permissive temperature of pIMAY), overnight. These cells were next inoculated into fresh medium and grown at 37 ^{O}C (non-permissive temperature of pIMAY), overnight. No growth was observed.

- Lower integration temperature: the colonies were inoculated into BHI supplemented with chloramphenicol 10 µg mL^{-1}, and grown at 33 or 35 ^{O}C, overnight. Cells showed growth when cultured at 33 ^{O}C. To select cells that have integrated the plasmid into their chromosome, these cultures were plated on TSA and the resulting colonies were screened by colony PCR, using the MCS oligonucleotides of pIMAY. The results showed that none of the colonies

screened kept the extrachromosomal plasmid. These colonies were further screened by colony PCR using oligonucleotides specific for the flanking regions of *hmp*. This PCR did not yield any product (Figure III.13), showing that integration did not occur. In total, 15 colonies were screened.

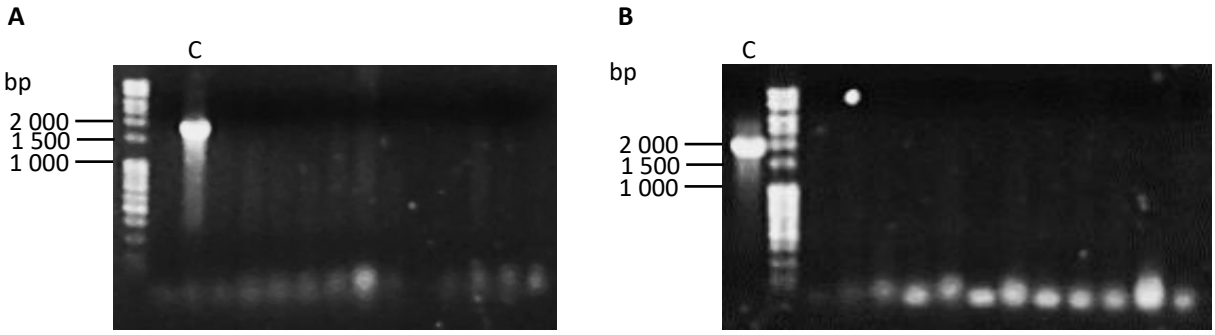

Figure III.13. Confirmation of the integration of pIMAY-*hmp*500 into the chromosome of *S. epidermidis* RP62A. After confirming the presence of the extrachromosomal plasmid, integration into the chromosome was induced by overnight growth at 33 ^{O}C. To confirm the integration, colony PCR was performed using the oligonucleotides hmp_D/hmp_out_fwd (A) and hmp_A/hmp_out_rev (B). The expected size of the amplicons is ~1 140 bp. (1) A colony of *S. epidermidis* RP62A was used as a positive control (C). The expected size of the amplicon is ~2 290 bp. Electrophoresis was performed in a 1% agarose gel, at 80 V.

In view of the non-obtention of the mutant, we resorted to another method. In this, we considered that longer flanking regions, *i.e.*, longer sequences for recombination, could improve the integration of the plasmid into the chromosome and, for that, another recombinant plasmid was constructed: pIMAY-*hmp*800. The flanking regions cloned into this plasmid are approximately 800 bp long, while the ones cloned into pIMAY-*hmp*500 are approximately 500 bp long. To introduce this plasmid into *S. epidermidis*, 10 electroporation experiments were performed over the course of 4 months, varying the following parameters:

- Intermediate cloning strain: *E. coli* DC10B or *S. aureus* RN4220 (see Appendix VI.7.2)
- Quantity of plasmid DNA: 1.2 – 8.7 µg
- Electroporation cuvette gap width: 1 and 2 mm
- Electroporation pulse voltage: 1.0 – 2.5 kV
- Electroporation recovery medium: TSB and SMMP

However, electroporation of *S. epidermidis* RP62A with this plasmid was not successful. Given that *S. epidermidis* 1457 is described in the literature has being more amenable to genetic manipulation than strain RP62A [16], construction of knock-out mutants was also attempted in this strain. *S. epidermidis* 1457 was transformed with pIMAY-*hmp*500, pIMAY-*hmp800* and pIMAY-*ric*500,

isolated from both *E. coli* DC10B and *S. aureus* RN4220. However, these transformations were not successful. Since electroporation of *S. epidermidis* is also hindered by its tendency to aggregate [79], electroporation of these plasmids into *S. epidermidis* 1457-M12, a biofilm-negative transposon mutant, was also tested. However, these transformations were also unsuccessful.

Thus, in spite of several attempts, construction of *S. epidermidis hmp* and *ric* knock-out strains was not successful. More alternative approaches are currently being addressed.

IV. Discussion

IV.1. Behavior of *Staphylococcus* under oxidative and nitrosative stress

Staphylococcus epidermidis and *S. aureus* are major constituents of the human microbiota, specially of the skin [4]. However, they are also important nosocomial pathogens, being highly associated with infections of implanted medical devices [24]. These infections are usually persistent and difficult to treat due to biofilm formation on the surface of the medical device. In this sessile state, bacteria are less susceptible to antibiotics and to the host immune system [6].

After the implantation of medical devices, the biomaterial triggers a local tissue response and macrophages are the main immune cell type to migrate to the tissue-biomaterial interface [80]. Professional phagocytes of innate immunity, like macrophages, produce cytotoxic compounds such as reactive oxygen species (ROS) and reactive nitrogen species (RNS), which interfere with several microbial targets with key cellular functions [53]. Nonetheless, pathogens have evolved defense mechanisms to survive in the hostile host environment. Some of these mechanisms have been unveiled for *S. aureus*, which is known to be highly resistant to oxidative and nitrosative stress [75, 76], while those of *S. epidermidis* remain largely unknown.

Therefore, we sought to investigate the resistance of *S. epidermidis* to oxidative and nitrosative stress, in its planktonic and biofilm forms, which correspond to the states found in the bloodstream and at the surface of implanted medical devices, respectively. Assays were performed under different oxygen concentrations to mimic the conditions encountered by pathogens during infection. The response of *S. aureus* biofilms to nitrosative stress was also analyzed.

IV.1.1. Oxidative stress: effect on planktonic cells and biofilms

Planktonic cells of *S. epidermidis* RP62A treated with concentrations of H_2O_2 up to 20 mM, at the early exponential phase of growth (OD_{600} of 0.4), were found to be highly resistant to oxidative stress (Figure III.1.A-B). Under aerobic conditions, a slight decrease in the growth of *S. epidermidis* was observed, while no significant effect was detected under microaerobic conditions.

Transcriptomic analyses of cells exposed to oxidative stress have been performed for *S. aureus* but not for *S. epidermidis*. In 2006, Chang and colleagues observed that, under aerobic conditions, a concentration of 10 mM hydrogen peroxide inhibited growth of *S. aureus* NCTC 8325 for 10 minutes, after which cells continued to grow at the same rate as untreated cells [76]. Our results are in agreement with this observation, in the sense that, after treatment with H_2O_2, *S. epidermidis* cells exposed to stress resumed growth at a similar rate to that of untreated cells.

Chang and colleagues also reported that the oxidative stress imposed by 10 mM H_2O_2 induced the expression of several genes, mainly involved in virulence, DNA repair and anaerobic metabolism. Notably, RIC and a putative flavohemoprotein were upregulated by ~6 and 4-fold, respectively. After 20 minutes of stress, when cells treated with H_2O_2 were already growing at the same rate as the untreated cells, the fold increase in the expression of these genes was found to be of ~9 and 10, respectively. Not only do these genes make part of the oxidative response of *S. aureus* but *ric* has also been demonstrated to be important for the oxidative stress resistance of *S. aureus* [69], while *hmp* has been implicated in the oxidative stress resistance of *E. coli* [81]. Since the genome of *S. epidermidis* RP62A encodes homologues of RIC and flavohemoglobin with high amino acid sequence identity to those of *S. aureus* and *E. coli,* it is reasonable to consider that these proteins also contribute to the protection of *S. epidermidis* against oxidative stress.

Later, in 2012, Nobre and Saraiva reported a transcriptomic study on the same strain of *S. aureus* as Chang and colleagues but grown under microaerobic conditions [82]. In this study, it was observed that oxidative stress imposed by 10 mM of hydrogen peroxide caused an alteration of the transcription levels of genes mainly involved in ROS detoxification, transport and binding, and DNA, energy and iron metabolisms. In particular, after 10 minutes of stress, catalase and superoxide dismutase were upregulated by ~4-fold. Therefore, as *S. epidermidis* RP62A also encodes catalase and superoxide dismutase, which are well known for their role in ROS detoxification [83], these enzymes may also contribute to its protection against oxidative stress, under microaerobic conditions.

Our data shows that, in general, the biofilm production of *S. epidermidis* RP62A and 1457 decreased with increasing concentrations of hydrogen peroxide (2 - 40 mM H_2O_2). It was also revealed that biofilms of *S. epidermidis* 1457 are more susceptible to oxidative stress than those of strain RP62A (Figures III.5 and III.7). This difference in susceptibility was more pronounced when cells were exposed to stress before establishment of the biofilm (Figures III.5.A and III.7.A): for instance, whereas concentrations of hydrogen peroxide up to 5 mM did not significantly affect the amount of biofilm produced by *S. epidermidis* RP62A, 5 mM H_2O_2 decrease the biofilm formation of strain 1457 by approximately half.

Both *S. epidermidis* strains encode identical catalase, superoxide dismutase, flavohemoglobin and RIC proteins. Therefore, the difference observed in the resistance to oxidative stress may be due to the presence of additional defense mechanisms or in differences in biofilm structure, namely regarding the composition of the extracellular matrix in which the cells are enclosed, which consequently affects the diffusion rate of substances like hydrogen peroxide. However, these questions have not yet been addressed in the literature.

In 2008, Glynn and colleagues reported a study on the effect of hydrogen peroxide on the biofilm development of *S. epidermidis* CSF41498 [84], a biofilm-forming strain isolated from cerebrospinal fluid [85]. According to their data, *S. epidermidis* CSF41498 and RP62A share the same nucleotide sequence regarding the *icaADBC* operon and exhibit similar biofilm-forming capacities when cultured in BHI. The *icaADBC* operon encodes for the enzymes required for the biosynthesis of the polysaccharide intercellular adhesion (PIA) [86], which is important for biofilm development [87]. Glyn and colleagues determined that the minimum inhibitory concentration of H_2O_2 for *S. epidermidis* CSF41498 was 18 mM, and that 5 and 10 mM of H_2O_2 caused a ~25% reduction in the biofilm capacity of this strain, when cells were exposed to stress before biofilm establishment and grown overnight. It was also observed that this reduction in biofilm production was accompanied by a down-regulation of *icaADBC* (the expression levels of *icaA* were decreased by over 3-fold) and an upregulation of *icaR*, which encodes a repressor of *icaADBC* [85]. In the 2006 transcriptomic study performed by Chang and colleagues [76], the genes that comprise the *ica* operon were also found to be down regulated by ~3-fold, in cells of *S. aureus* exposed to 10 mM of hydrogen peroxide.

While for *S. epidermidis* CSF41498 it was reported that 5 and 10 mM of H_2O_2 caused a decrease in biofilm formation of ~25%, in our work the same concentrations of stress induced a reduction of ~14% and ~79% for strain RP62A, and of ~51% and 71% for strain 1457, respectively. However, the experimental conditions were different: after application of the oxidative stress, *S. epidermidis* CSF41498 was grown overnight, while we cultured the cells for only 8 hours. Moreover, as our data suggests, *S. epidermidis* is able to recover biofilm production over time. Therefore, one may consider that the smaller decreases in biofilm production observed for CSF41498 are due to the fact that these cells were cultured for a long time, which allow them to recover from the stress imposed. Moreover, it is possible that the same mechanism of down-regulation of the *ica* operon, through an up-regulation of *icaR*, is involved in the decrease of biofilm production observed in this work for RP62A and 1457 exposed to oxidative stress.

IV.1.2. Nitrosative stress: effect on planktonic cells, biofilms and expression levels of flavohemoglobin (*hmp*) and repair of iron centers (*ric*)

In the planktonic state, it was observed that concentrations of GSNO up to 200 µM did not affect the growth of *S. epidermidis* RP62A, while 800 µM caused a severe growth impairment, independent of the oxygen growth conditions (Figure III.1.E-F). Since GSNO not only acts as a NO-donor but also as a nitrosating agent, the growth behavior or *S. epidermidis* RP62A was also evaluated under nitrosative stress induced by spermine-NONOate (Figure III.1.C-D), which acts solely as a NO-donor. The same effect on the growth of *S. epidermidis* was observed when nitrosative stress was induced with the same concentration (200 µM) of GSNO and spermine-NONOate.

A previous study addressed the effect of GSNO-induced nitrosative stress on the growth behavior of *S. aureus* RN4220 [88]. Consistent with our data, concentrations of GSNO up to 200 µM did not affect the growth of *S. aureus* under microaerobic conditions. However, while 200 µM GSNO strongly inhibited the growth of *S. aureus* under aerobic conditions, the same was not observed for *S. epidermidis*. Gonçalves and colleagues also demonstrated that, whereas the growth of the *S. aureus* wild type strain was not affected by 200 µM GSNO under microaerobic conditions, the growth of a flavohemoglobin knock-out mutant was significantly impaired, suggesting a protective role for this protein under these conditions. Moreover, it was shown that the expression of flavohemoglobin (*hmp*) was induced by oxygen-limited growth conditions and it was not further enhanced by NO.

Contrary to this study, our qRT-PCR data revealed that in *S. epidermidis* RP62A the *hmp* gene is more upregulated under aerobic conditions (~4-fold) than microaerobic conditions (~3-fold), after stress imposed by 200 µM of spermine-NONOate. This data suggests that *hmp* is differently regulated in both bacteria and that flavohemoglobin may contribute to the aerobic protection of *S. epidermidis* against nitrosative stress. Our qRT-PCR data also revealed a similar upregulation of *ric*, which has been demonstrated to be highly upregulated in *S. aureus* JE2 during infection of *Galleria mellonella* [69].

A transcriptomic study performed on *S. aureus* NCTC 8325 grown in microaerobic conditions revealed that nitrosative stress induced by 150 µM of GSNO caused the upregulation of genes mainly encoding proteins involved in transport and binding and energy metabolism, similarly to what has been observed for H_2O_2-induced stress [83]. GSNO-induced stress also altered the expression levels of genes with regulatory functions, such as *srrA*, which was downregulated by ~2-fold. SrrA is involved in the regulation of virulence factors and represses the accessory gene regulator (*agr*), the toxic shock syndrome toxin gene (*tst*) and the gene for protein A (*spa*). The expression of genes encoding proteins important for nitrosative stress resistance was also induced, such as *ntrA* [89].

In this work, we also investigated the behavior of biofilms of *S. epidermidis* and *S. aureus* upon nitrosative stress, at different moments of the biofilm development process. Resembling what was observed for oxidative stress, biofilms of *S. epidermidis* 1457 exhibited a higher susceptibility to nitrosative stress than those of strain RP62A, which was more pronounced when the stress was applied before cell adherence (Figures III.5 and III.7). Whereas 50 µM GSNO did not affect the biofilm formation of *S. epidermidis* RP62A, the same concentration of stress led to a decrease of ~55% of the biomass of biofilm produced by strain 1457.

When nitrosative stress was applied to already established biofilms, both strains were found to be highly resistant to stress. Biofilm quantification after the cells were allowed to recover for 3 hours, showed that concentrations of GSNO of 50 to 800 µM induced similar effects on biofilm production, with a decrease of ~20% for RP62A and of ~25% for 1457. On the other hand, 1 mM GSNO caused a more pronounced decrease in biofilm formation (~57% and ~75% for RP62A and 1457, respectively).

Biofilms of *S. aureus* JE2, a strain derived from the highly characterized CA-MRSA strain USA300 LAC by curing of three plasmids, were also studied. This strain is a weaker biofilm producer than the strains of *S. epidermidis* studied, as ascertained by quantification of biofilm biomass by staining with 1% (v/v) crystal violet and absorbance measurement at 570 nm: on average, after 8 hours of growth, values of ~2 were obtained for the *S. epidermidis* strain, while *S. aureus* JE2 yielded values of ~0.5.

Contrary to what was observed for *S. epidermidis*, exposure to nitrosative stress exerted a greater effect of the biofilm formation capacity on *S. aureus* JE2 when stress was applied to already established biofilms, rather than to cells not yet adherent. While treatment with 200 µM of GSNO prior to adherence did not affect the amount of biofilm produced by *S. aureus*, the same concentration of stress induced a ~26% decrease in biofilm formation when applied to 4-hour old biofilms (Figure III.8.B). However, when stress was induced with 500 µM of GSNO before attachment and cells were grown for 24 hours, an unexpected increase of ~45% was observed in the biofilm formation of *S. aureus* JE2. The observed increase in biofilm production could be part of the defense response of *S. aureus* to a higher nitrosative stress, i.e., in the presence of a higher stress the biofilm formation of *S. aureus* might have been enhanced as a protective mechanism. On the other hand, the initial adaptation response to the stress could have involved an alteration at the transcriptional and metabolic levels that, in the long term, enhanced the fitness of these cells.

Biofilms of flavohemoglobin and RIC knock-out mutants were also analyzed, to determine the importance of these proteins in the response to nitrosative stress. The *S. aureus* Δ*ric* strain exhibited a similar phenotype to the parent strain in all the conditions tested, which indicates that this protein is not essential for nitrosative stress resistance. On the contrary, deletion of *hmp* abrogated the effect

of nitrosative stress, except for higher concentrations and long times of exposure. This data suggests that flavohemoglobin is important for the protection of *S. aureus* against high levels of nitrosative stress. However, further experiments are required to optimize the protocol for biofilm assays in *S. aureus* to confirm the significance of these results.

IV.2. Construction of *S. epidermidis* knock-out strains

Despite several attempts, the construction of *S. epidermidis hmp* and *ric* knock-out strains by allelic replacement mutagenesis was not successful. When recombinant plasmids for allelic replacement were designed with flanking regions of ~500 bp, we were able to transform these plasmids into *S. epidermidis* but integration into the chromosome was not achieved. Considering that longer sequences for recombination would improve the chromosomal integration of the plasmid [90, 91], flanking regions of ~800 bp were cloned into a new recombinant plasmid. However, transformation of *S. epidermidis* with this new plasmid was not successful.

In addition to the thick peptidoglycan layer of the cell wall [92, 93] of *S. epidermidis*, its strong modification-restriction systems further difficult its transformation. It is thought that the type IV restriction enzyme McrR, which recognizes cytosine-methylated DNA, is the major barrier to *S. epidermidis* transformation [78]. To bypass this barrier, two intermediate cloning strains were used: *S. aureus* RN4220 and *E. coli* DC10B. *S. aureus* RN4220 has premature stop codons in the genes that encode for the restriction enzymes SauUSI (ortholog of McrR) and HsdR, which makes this strain able to modify but not restrict foreign DNA [74]. Thus, passage of *E. coli* derived DNA through RN4220 allows the transformation of closely related staphylococcal strains. The strain *E. coli* DC10B was generated by deletion of the gene encoding for the DNA-cytosine methyltransferase (*dcm*) of *E. coli* DH10B (high-efficiency cloning strain), with the purpose to create a universal staphylococcal cloning host [74]. Although we used both intermediate cloning strains, transformation of *S. epidermidis* was still very difficult. Further experiences are being designed to overcome this issue.

V. Conclusion

Staphylococcus epidermidis and *Staphylococcus aureus* are major constituents of the human microbiota but also serious nosocomial pathogens. These bacteria are able to establish biofilms that are inherently resistant to antimicrobial agents and to the host immune system, which hampers treatment of related infections. The development of new therapeutic strategies to control these infections requires a deeper understanding of the resistance mechanisms of these pathogens. To survive in the host, *S. epidermidis* and *S. aureus* must cope with the hostile conditions created by the immune system, including the oxidative and nitrosative stresses imposed by professional phagocytes of innate immunity. Some of the mechanisms that allow *S. aureus* to thrive under these conditions have been studied, but it remains a poorly explored topic regarding *S. epidermidis*.

In this work, the resistance of *S. epidermidis* and *S. aureus* against oxidative and nitrosative stresses was evaluated and compared by determining the growth rate of planktonic cells and the amount of biofilm produced, under stress conditions. It was shown that *S. epidermidis* is highly resistant to these stresses, in its planktonic and biofilm states, regardless of the oxygen growth conditions. Moreover, data revealed that its biofilm-producing capacity was more compromised when stress was applied prior to biofilm establishment, and that it is able to recover this capacity over time. The opposite was observed for *S. aureus*, which was more susceptible to nitrosative stress when this was applied to established biofilms.

Flavohemoglobin (Hmp) and repair of iron centers (RIC) are proteins involved in stress detoxification and repair, and their protective role in planktonic cells of *S. aureus* is well established. Herein, it was observed that deletion of *ric* did not affect the response of *S. aureus* biofilms to nitrosative stress. On the other hand, deletion of *hmp* restored the levels of biofilm formation to those of untreated cells, for low concentrations of stress, but enhanced the susceptibility to high concentrations of stress during long periods of exposure. Furthermore, it was determined that *hmp* and *ric* are upregulated in planktonic cells of *S. epidermidis* exposed to nitrosative stress. Altogether, these results indicate a role for these proteins in stress survival.

Further studies are necessary to confirm and complement the data obtained in this work. The protocol for biofilm assays requires further optimization for *S. aureus*, to ascertain the significance of the results obtained. To assess the role of *hmp* and *ric* in the survival of *S. epidermidis* to stress, new

strategies to construct knock-out mutants need to be explored, namely resorting to phage technology. It would also be interesting to study these mutants in infections models, such as macrophages cultures. Considering that flavohemoglobin and RIC prove to be important for the resistance of *S. epidermidis*, their biochemical characterization would be useful to rationalize their protective role. To further elucidate the transcriptomic events underlying the defenses responses triggered by stress exposure, RNA sequencing assays of biofilms cells of *S. epidermidis* and *S. aureus* are also important studies to be performed in the future.

Bibliography

1. Brooks, G. *et al.* (2013) ***Medical Microbiology***. 26th Edition. McGraw-Hill.
2. Rogers, K. *et al*. (2009) **Coagulase-negative Staphylococcal Infections**. *Infectious Disease Clinics of North America*, 23(1), pp.73-98.
3. Madigan, M. *et al*. (2012) ***Brock Biology of Microorganisms***. 13th Edition. Boston: Pearson.
4. Kloos, W. and Musselwhite, M. (1975) **Distribution and Persistence of *Staphylococcus* and *Micrococcus* Species and Other Aerobic Bacteria on Human Skin**. *Applied Microbiology*, 30(3), pp. 381-396.
5. Keyworth, N. *et al.* (1992) **Development of Cutaneous Microflora in Premature Neonates**. *Archives of Disease in Childhood*, 67, pp. 797-801.
6. Wilson, B. *et al*. (2011) ***Bacterial Pathogenesis – A Molecular Approach***. 3rd Edition. Washington DC: ASM Press.
7. Otto, M. (2009) ***Staphylococcus epidermidis* – The «Accidental» Pathogen**. *Nature Reviews Microbiology*, 7(8), pp. 555-567.
8. Cheung, G. *et al.* (2014) **Phenol-soluble Modulins – Critical Determinants of Staphylococcal Virulence**. *FEMS Microbiology Reviews*, 38(4), pp. 698-719.
9. Fey, P. (2014) ***Staphylococcus epidermidis – Methods and Protocols***. Human Press.
10. Shore, A. & Coleman, D. (2013) **Staphylococcal Cassette Chromosome *mec*: Recent Advances and Insights**. *International Journal of Medical Microbiology*, 303, pp. 350-359.
11. Ito, T. *et al.* (2014) **Staphylococcal Cassette Chromosome *mec* (SCC*mec*) Analysis of MRSA.** In: Ji, Y. (Ed) *Methicillin-resistant Staphylococcus aureus (MRSA) Protocols*. Vol. 1085. 2nd Edition. Springer.
12. Christensen, G. *et al.* (1982) **Nosocomial Septicemia Due to Multiply Antibiotic-resistant *Staphylococcus epidermidis*.** *Annals of Internal Medicine*, 96(1), pp. 1-10.
13. Gill, S. *et al.* (2005) **Insights on Evolution of Virulence and Resistance from the Complete Genome Analysis of an Early Methicillin-Resistant *Staphylococcus aureus* Strain and a Biofilm-Producing Methicillin-Resistant *Staphylococcus epidermidis* Strain.** *Journal of Bacteriology*, 187(7), pp. 2426-2438.
14. Mack, D. *et al*. (1992) **Parallel Induction by Glucose of Adherence and a Polysaccharide Antigen Specific for Plastic-adherent *Staphylococcus epidermidis*: Evidence for Functional Relation to Intercellular Adhesion.** *Infection and Immunity*, 60(5), pp. 2048-2057.
15. Mack, D. *et al.* (2002) **Differential Expression of Methicillin Resistance by Different Biofilm-negative *Staphylococcus epidermidis* Transposon Mutant Classes**. *Antimicrobial Agents and Chemotherapy*, 46(1), pp. 178-183.
16. Galac, M. *et al.* (2017) **Complete Genome Sequence of *Staphylococcus epidermidis* 1457.** *Genome Announcements*, 5(22), e00450-17.
17. Ogston, A. (1882) **Micrococcus Poisoning.** *Journal of Anatomy and Physiology*, 17, pp. 24-58.
18. Tong, S. *et al.* (2015) ***Staphylococcus aureus* Infections: Epidemiology, Pathophysiology, Clinical Manifestations, and Management.** *Clinical Microbiology Reviews*, 2883), pp. 603-661.
19. Fitzgerald, J. (2014) **Evolution of *Staphylococcus aureus* During Human Colonization and Infection.** *Infection, Genetics and Evolution*, 21, pp. 542-547.
20. Wertheim, H. (2005) **The Role of Nasal Carriage in *Staphylococcus aureus*.** *The Lancet Infectious Diseases*, 5(12), pp. 751-762.
21. Colon, B. (2014) ***Staphylococcus aureus* Chronic and Relapsing Infections: Evidence of a Role for Persister Cells.** *Bioessays*, 36(10):991-6.
22. Enright, M. *et al.* (2002) **The Evolutionary History of Methicillin-resistant *Staphylococcus aureus* (MRSA).** *PNAS*, 99(11), pp. 7687-7692.
23. Figueiredo, A. *et al.* (2017) **The Role of Biofilms in Persistent Infections and Factors Involved in *ica*-independent Biofilm Development and Gene Regulation in *Staphylococcus aureus*.** *Critical Reviews in Microbiology*, 43(5), pp. 602-620.

24. Arciola, C., Campoccia, D. and Montanaro, L. (2018) **Implant Infections: Adhesion, Biofilm Formation and Immune Evasion.** *Nature Reviews Microbiology*, 16, pp. 397-409.

25. Archer, N. *et al.* (2011) ***Staphylococcus aureus* Biofilms: Properties, Regulation and Roles in Human Disease.** *Virulence*, 2(5), pp. 445-459.

26. Lister, J. and Horswill, A. (2014) ***Staphylococcus aureus* Biofilms: Recent Developments in Biofilm Dispersal.** *Frontiers in Cellular and Infection Microbiology*, 4:178.

27. Águilla-Arcos, S. *et al.* (2017) **Biofilm-forming Clinical *Staphylococcus* Isolates Harbor Horizontal Transfer and Antibiotic Resistance Genes.** *Frontiers in Microbiology*, 8:2018.

28. Nesse, L. and Simm, R. (2018) **Biofilm: A Hotspot for Emerging Bacterial Genotypes.** In: Sariaslani, S. and Gadd, G. (Eds.) *Advances in Applied Microbiology*, Vol. 103. Elsevier Academic Press.

29. Houte, S., Buckling, A., and Westra, E. (2016) **Evolutionary Ecology of Prokaryotic Immune Mechanisms.** *Microbiology and Molecular Biology Reviews*, 80(3), pp. 745-763.

30. Horvath, P. and Barrangou, R. (2010) **CRISPR/Cas, the Immune System of Bacteria and Archaea.** *Science*, 327, pp. 167-170.

31. Abbas, A. *et al.* (2015) ***Cellular and Molecular Immunology***. 8th Edition. Philadelphia: Elsevier Saunders.

32. Romo, M., Pérez-Martínez, D., and Ferrer, C. (2016) **Innate Immunity in Vertebrates: An Overview.** *Immunology*, 148, pp. 125-139.

33. Zimmerman, L. *et al.* (2009) **Understanding the Vertebrate Immune System: Insights from the Reptilian Perspective.** *The Journal of Experimental Biology*, 213, pp. 661-671.

34. Magnadóttir, B. (2006) **Innate Immunity of Fish (Overview).** *Fish & Shellfish Immunology*, 20, pp. 137-151.

35. Cerenius, L. *et al*. (2010) **Crustacean Immunity**. In: Söderhäll, K. (ed.) *Invertebrate Immunity*. Advances in Experimental Medicine and Biology, vol. 708. Boston: Springer.

36. Juul-Madsen, H. *et al.* (2008) **Avian Innate Immune Responses.** In: Davison, F., Kaspers, B., and Schat, K. (eds.) *Avian Immunology*. London: Elsevier.

37. Jones, J. and Dangl, J. (2006) **The Plant Immune System**. *Nature*, 444, pp. 323-329.

38. Dodds, P. and Rathjen, J. (2010) **Plant Immunity: Towards an Integrated View of Plant-pathogen Interactions.** *Nature Reviews Genetics*, 11, pp. 539-548.

39. Müller, U. *et al.* (2008) **The Innate Immune System of Mammals and Insects.** *Trends in Innate Immunity*, 15, pp. 21-44.

40. Vilmos, P. and Kuruez, É. (1998) **Insect Immunity: Evolutionary Roots of the Mammalian Innate Immune System.** *Immunology Letters*, 62, pp. 59-66.

41. Uehling, J. *et al.* (2017) **Do Fungi Have an Innate Immune Response? An NLR-based Comparison to Plant and Animal Immune Systems.** *PLoS Pathogens*, 13(10), e1006578.

42. Cooper, M. and Alder, M. (2006) **The Evolution of Adaptive Immune Systems**. *Cell*, 124, pp. 815-822.

43. Flajnik, M. and Kasahara, M. (2010) **Origin and Evolution of the Adaptive Immune System: Genetic Events and Selective Pressures.** *Nature Reviews Genetics*, 11(1), pp. 47-59.

44. Akira, S., Uematsu, S., and Takeuchi, O. (2006) **Pathogen Recognition and Innate Immunity.** *Cell*, 124, pp. 783-801.

45. Beutler, B. (2004) **Innate Immunity: An Overview.** *Molecular Immunology*, 40, pp. 845-859.

46. Papayannopoulos, V. (2018) **Neutrophil Extracellular Traps in Immunity and Disease.** *Nature Reviews Immunology*, 18, pp. 134-147.

47. Kolaczkowska, E. and Kubes, P. (2013) **Neutrophil Recruitment and Function in Health and Inflammation.** *Nature Reviews Immunology*, 13, pp. 159-175.

48. Geissmann, F. *et al.* (2010) **Development of Monocytes, Macrophages and Dendritic Cells.** *Science*, 327, pp.656-661.

49. Kumar, V., Abbas, A., and Aster, J. (2013) ***Robbins Basic Pathology.*** 9th Edition. Philadelphia: Elsevier Saunders.

50. Botelho, R. and Grinstein, S. (2011) **Phagocytosis.** *Current Biology*, 21(14), pp. R533-538.

51. Aderem, A. (2003) **Phagocytosis and the Inflammatory Responses.** *Journal of Infectious Diseases*, 187, pp. S-340-345.

52. Goldsby, R. *et al.* (2003) ***Immunology*.** 5th Edition. New York: W. H. Freeman.

53. Fang, F. (2004) **Antimicrobial Reactive Oxygen and Nitrogen Species: Concepts and Controversies.** *Nature Reviews Microbiology*, 2, pp. 820-832.

54. Wajcman, H., Kiger, L. and Marden, M. (2009) **Structure and Function Evolution in the Superfamily of Globins**. *Comptes Rendus Biologies,* 332, pp. 273-282.

55. Tejero, J. and Gladwin, M. (2014) **The Globin Superfamily: Functions in Nitric Oxide Formation and Decay.** *Biological Chemistry*, 395(6), pp. 631-639.

56. Poole, R. (2005) **Nitric Oxide and Nitrosative Stress Tolerance in Bacteria.** *Biochemical Society Transactions*, 33(1), pp. 176-180.

57. Poole, R. and Hughes, M. (2000) **New Functions for the Ancient Globin Family: Bacterial Responses to Nitric Oxide and Nitrosative Stress.** *Molecular Microbiology*, 36(4), pp. 775-783.

58. Bonamore, A. and Boffi, A. (2008) **Flavohemoglobin: Structure and Reactivity.** *IUBMB Life*, 60(1), pp. 19-28.

59. Forrester, M. and Foster, M. (2012) **Protection from Nitrosative Stress: A Central Role for Microbial Flavohemoglobin.** *Free Radical Biology & Medicine*, 52, pp. 1620-1633.

60. Justino, M. *et al.* (2005) **New Genes Implicated in the Protection of Anaerobically Grown *Escherichia coli* Against Nitric Oxide.** *The Journal of Biological Chemistry*, 280(4), pp. 2636-2643.

61. Nobre, L. *et al.* (2014) ***Escherichia coli* RIC is Able to Donate Iron to Iron-sulfur Clusters.** *PLoS ONE*, 9(4): e95222.

62. Mukhopadhyay, P. *et al.* (2004) **Prominent Roles of the NorR and Fur Regulators in the *Escherichia coli* Transcriptional Response to Reactive Nitrogen Species.** *PNAS*, 101(3), pp. 745-750.

63. Justino, M. *et al.* (2006) ***Escherichia coli* YtfE is a Di-iron Protein with an Important Function in Assembly of Iron-sulphur Clusters**. *FEMS Microbiology Letters*, 257, pp. 278-284.

64. Justino, M., Baptista, J., and Saraiva, L. (2009) **Di-iron Proteins of the Ric Family are Involved in Iron-sulfur Cluster Repair.** *Biometals*, 22, pp. 99-108.

65. Nobre, L. *et al.* (2015) **Insights into the Structure of the Diiron Site of RIC from *Escherichia coli*.** *FEBS Letters*, 589, pp. 426-431.

66. Lo, F. *et al.* (2016) **Crystal Structure Analysis of the Repair of Iron Centers Protein YtfE and Its Interaction with NO.** *Chemistry – A European Journal*, 22, pp. 9768-9776.

67. Justino, M. *et al.* (2007) ***Escherichia coli* Di-iron YtfE Protein is Necessary for the Repair of Stress-damaged Iron-Sulfur Clusters.** *The Journal of Biological Chemistry*, 282(14), pp. 10352-10359.

68. Overton, T. *et al.* (2008) **Widespread Distribution in Pathogenic Bacteria of Di-iron Proteins that Repair Oxidative and Nitrosative Damage to Iron-sulfur Centers.** *Journal of Bacteriology*, 190(6), pp. 2004-2013.

69. Silva, L. *et al.* (2017) **Repair of Iron Centers RIC Protein Contributes to the Virulence of *Staphylococcus aureus*.** *Virulence*, 9(1), pp. 312-317.

70. Christensen, G. *et al.* (1985) **Adherence of Coagulase-negative Staphylococci to Plastic Tissue Culture Plates: A Quantitative Model for the Adherence of Staphylococci to Medical Devices.** *Journal of Clinical Microbiology*, 22(6), pp. 996-1006.

71. Baldassarri, L. *et al.* (1993) **Variable Fixation of Staphylococcal Slime by Different Histochemical Fixatives.** *European Journal of Clinical Microbiology & Infectious Diseases*, 12, pp. 866-868.

72. Xu, T. *et al.* (2017) **Identification of Genes Controlled by the Essential YycFG Two-component System Reveals a Role for Biofilm Modulation in *Staphylococcus epidermidis*.** *Frontiers in Microbiology*, 8:724.

73. Livak, K. and Schmittgen, T. (2001) **Analysis of Relative Gene Expression Data Using Real-time Quantitative PCR and the $2^{-\Delta\Delta CT}$ Method.** *Methods*, 25, pp.402-408.

74. Monk, I. *et al.* (2012) **Transforming the Untransformable: Application of Direct Transformation to Manipulate Genetically *Staphylococcus aureus* and *Staphylococcus epidermidis*.** *mBio*, 3(2), e00277-11.

75. Richardson, A., Dunman, P. and Fang, F. (2006) **The Nitrosative Stress Response of *Staphylococcus aureus* is Required for Resistance to Innate Immunity.** *Molecular Microbiology*, 61(4), pp. 927-939

76. Chang, W. *et al.* (2006) **Global Transcriptome Analysis of *Staphylococcus aureus* Response to Hydrogen Peroxide.** *Journal of Bacteriology*, 188(4), pp. 1648-1659.

77. Nobre, L., Gonçalves, V. and Saraiva, L. (2008) **Flavohemoglobin of *Staphylococcus aureus*.** In: Poole, R. (Ed.) *Methods in Enzymology,* vol. 436. Academic Press.

78. Monk, I. and Foster, T. (2012) **Genetic Manipulation of Staphylococci – Breaking Through the Barrier.** *Frontiers in Cellular and Infection Microbiology*, 2, 1-9.

79. Maliszewski, K. and Nuxoll, A. (2014) **Use of Electroporation and Conjugative Mobilization for Genetic Manipulation of *Staphylococcus epidermidis*.** In: Fey, P. (Ed.) *Staphylococcus epidermidis*: Methods and Protocols, vol. 1106. Springer.

80. Park, K. and Bryers, J. (2012) **Effect of Macrophage Classical (M1) Activation on Implant-adherent Macrophage Interactions with *Staphylococcus epidermidis*: A Murine *in vitro* Model System.** *Journal of Biomedical Materials Research*, 100A(8), pp. 2045–2053.

81. Membrillo-Hernández, J. *et al.* (1999) **The Flavohemoglobin of *Escherichia coli* Confers Resistance to a Nitrosating Agent, a "Nitric Oxide Releaser" and Paraquat and is Essential for Transcriptional Responses to Oxidative Stress.** *The Journal of Biological Chemistry*, 274(2), pp. 748-754.

82. Nobre, L. and Saraiva, L. (2013) **Effect of Combined Oxidative and Nitrosative Stresses on *Staphylococcus aureus* Transcriptome.** *Applied Microbiology and Biotechnology*, 97, pp. 2563-2573.

83. Gaupp, R., Ledala, N., and Somerville, G. (2012) **Staphylococcal Response to Oxidative Stress.** *Frontiers in Cellular and Infection Microbiology*, 2:33.
84. Glynn, A. *et al.* (2009) **Hydrogen Peroxide Induced Repression of *icaADBC* Transcription and Biofilm Development in *Staphylococcus epidermidis*.** *Journal of Orthopaedic Research*, 27, pp. 627-630.
85. Conlon, K., Humphreys, H. and O'Gara, J. (2002) ***icaR* Encodes a Transcriptional Repressor Involved in Environmental Regulation of *ica* Operon Expression and Biofilm Formation in *Staphylococcus epidermidis*.** *Journal of Bacteriology*, 184(16), pp. 4400-4408.
86. Gerke, C. *et al*. (1998) **Characterization of the *N*-acetylglucosaminyltransferase Activity Involved in the Biosynthesis of the *Staphylococcus epidermidis* Polysaccharide Intercellular Adhesin.** *The Journal of Biological Chemistry*, 273(29), pp. 18586-18593.
87. Mack, D. *et al.* (1996) **The Intercellular Adhesin Involved in Biofilm Accumulation of *Staphylococcus epidermidis* is a Linear β-1,6-Linked Glycosaminoglycan: Purification and Structural Analysis.** *Journal of Bacteriology*, 178(1), pp.175-183.
88. Gonçalves, V. *et al.* (2006) **Flavohemoglobin Requires Microaerophilic Conditions for Nitrosative Protection of *Staphylococcus aureus*.** *FEBS Letters*, 580, pp. 1817-1821.
89. Pragman, A. *et al.* (2004) **Characterization of Virulence Factor Regulation by SrrAB, a Two-component System in *Staphylococcus aureus*.** *Journal of Bacteriology*, 186(8), pp. 2430-2438.
90. Watt, V. *et al.* (1985) **Homology Requirements for Recombination in *E. coli*.** *PNAS*, 82, pp. 4768-4772.
91. Kung, S. *et al.* (2013) **Effects of DNA Size on Transformation and Recombination Efficiencies in *Xylella fastidiosa*.** *Applied and Environmental Microbiology,* 79(5) pp. 1712-1717.
92. Dower, W. *et al*. (1991) **Protocols for the Transformation of Bacteria by Electroporation.** In: Chang, D. *et al.* (Eds.) *Guide to Electroporation and Electrofusion*. Elsevier.
93. Löfblom, J. *et al.* (2007) **Optimization of Electroporation-mediated Transformation: *Staphylococcus carnosus* as a model organism.** *Journal of Applied Microbiology*, 102, pp. 736-747.
94. Mandel, M. and Higa, A. (1970) **Calcium-dependent Bacteriopahge DNA Infection.** *Journal of Molecular Biology*, 53, pp. 159-162.
95. Froger, A. and Hall, J. (2007) **Transformation of Plasmid DNA into *E. coli* Using the Heat Shock Method.** *Journal of Visualized Experiments*, 6.
96. Kraemer, G. and Iandolo, J. (1990) **High-frequency Transformation of *Staphylococcus aureus* by Electroporation.** *Current Microbiology*, 21, pp. 373-376.
97. Grosser, M. and Richardson, A. (2016) **Method for Preparation and Electroporation of *S. aureus* and *S. epidermidis*.** *Methods in Molecular Biology*, 1353, pp. 51-57.

VI. Appendices

VI.1. Composition of culture media

Table VI.1. Composition of the culture media used in this work.

Component	Concentration	Purpose
Tryptic soy broth (TSB) - Supplied by *BD Difco ™*		
Tryptone	17 g L^{-1}	Liquid medium for routine culture
Soytone	3 g L^{-1}	of *Staphylococcus*
Glucose	2.5 g L^{-1}	
Sodium chloride (NaCl)	5 g L^{-1}	
Dipotassium hydrogen phosphate (K_2HPO_4)	2.5 g L^{-1}	
Brain-heart infusion broth (BHI) - Supplied by *Oxoid ™ Thermo Scientific ™*		
Brain infusion solids	12.5 g L^{-1}	Liquid medium for routine culture
Beef heart infusion solids	5 g L^{-1}	of *Staphylococcus*
Proteose peptone	10 g L^{-1}	
Glucose	2 g L^{-1}	
Sodium chloride (NaCl)	5 g L^{-1}	
Disodium phosphate (Na_2HPO_4)	2.5 g L^{-1}	
Luria-Bertani broth (LB) – Supplied by *Carl Roth ®*		
Tryptone	10 g L^{-1}	Liquid medium for routine culture
Yeast extract	5 g L^{-1}	of *E. coli*
Sodium chloride (NaCl)	10 g L^{-1}	
1X SMM buffer		
Sucrose	0.50 M	
Maleic acid	0.02 M	
Magnesium chloride hexahydrate ($MgCl_2 \bullet 6H_2O$)	0.02 M	
1X Penassay broth		
Beef extract	1.5 g L^{-1}	
Yeast extract	1.5 g L^{-1}	
Peptone	5 g L^{-1}	
Glucose	1 g L^{-1}	
Sodium chloride (NaCl)	3.5 g L^{-1}	
Dipotassium phosphate (K_2HPO_4)	3.68 g L^{-1}	
Monopotassium phosphate (KH_2PO_4)	1.32 g L^{-1}	
Sucrose maleate magnesium chloride penassay broth (SMMP)		Electroporation recovery medium
Mix equal parts of 2X SMM buffer and 4X Penassay broth		

To prepare solid culture media, agar was added at concentration of 15 g L^{-1}.

VI.2. Oligonucleotides and enzymes

The oligonucleotides used in this work are listed in Table VI.2.

Table VI.2. Oligonucleotides used in this work.

Oligonucleotide	Sequence (5' → 3')	Restriction Endonuclease
RT-PCR		
gyrB_fwd [72]	GCTAATGCCTCGTCAATAC	
gyrB_rev [72]	TATGGTGCTGGACAGATAC	
hmp_fwd	CAAGAAACAAGTGACATCAAATC	
hmp_rev	TCATGTTCAGTAGTCACATCAC	
ric_fwd	GAAGGTAACAGTACCATTAATCC	
ric_rev	TCCAACATACTATCACGAAACTC	
Confirmation of NARSA mutants		
NARSA_upstream	CTCGATTCTATTAACAAGGG	
NARSA_buster	GCTTTTTCTAAATGTTTTTTAAGTAAATCAAGTAC	
SA_hmp_up	TATACAGATTAAAGGAGGAGTACCATGGTTACAGAA	
SA_hmp_down	CGTTGATTAAGTTTCATATGAGCACGAATTCTCTTT	
SA_ric_up	GGCGAACCATACTTTAAAGGCATTGAT	
SA_ric_down	GGTCCATGTACTTTCGATAACTTC	
Construction of *S. epidermidis* deletion strains		
MCS_fwd	TACATGTCAAGAATAAACTGCCAAAGC	
MCS_rev	AATACCTGTGACGGAAGATCACTTCG	
hmp_out_fwd	CTCATCTTCTTTACGTATATGATCCAA	
hmp_out_rev	CCTCTAAAGGCTCACGAACC	
hmp_A	CGGAATTCGTGACTAGGACCATGTACTTTTGC	EcoRI
hmp_A2	CGCGGAATTCACATGTTGGTGTGTTTGACG	EcoRI
hmp_B	**CTCAGTTCCTTTATCTTGTA**ATAATGG	
hmp_C	**TACAAGATAAAGGAACTGAG**CATGTTCATTTTGAAACATTTATTCCTCGT	
hmp_D	GCGTCGACCCTCTGTATATTCTCTCTCTACCAGG	SalI
hmp_D2	CGCGGTCGACGGTAGAACGAGAACGTCTAAAC	SalI
ric_out_fwd	CCATAACATATGGTTGTAAATTTCTTG	
ric_out_rev	CATTTTCATAGAATAGATGCAGATGAAG	
ric_A	CGGAGCTCCCATGTTTGAATTACTGGGTC	SacI
ric_B	**TGTTACAACATCTGCAACAATATC**	
ric_C	**GATATTGTTGCAGATGTTGTAACA**CATGTACATCTTGAAAACCATGTG	
ric_D	GCGTCGACGGTGAATATCATACTGTTAAATTAGG	SalI

Underlined segments: recognition sequences for restriction endonucleases
Bold segments: complementary regions for splicing by overlap extension polymerase chain reaction (SOE-PCR)

The enzymes used in this work are listed in Table VI.3. When applicable, the enzymatic reactions were carried out in the buffers provided with the enzymes.

Table VI.3. Enzymes used in this work.

Enzyme	Restriction Site (5' → 3')	Supplier
Taq DNA Polymerase	NA	New England Biolabs
T4 DNA ligase	NA	New England Biolabs
Phusion high-fidelity DNA polymerase	NA	Thermo Fisher Scientific
EcoRI-HF	G|AATTC	New England Biolabs
SalI-HF	G|TCGAC	New England Biolabs
SacI	GAGCT|C	New England Biolabs
Lysozyme (from chicken egg white)	NA	Sigma
Lysostaphin (from *S. staphylolyticus*)	NA	Sigma

NA: not applicable
HF: high-fidelity

VI.3. Commercial kits, other reagents and solutions

All the commercial kits used in the course of this work are listed in Table IV.4. Unless stated otherwise, these kits were used as indicated by the manufacturer.

Table VI.4. Commercial kits used in this work.

Kit	Supplier	Purpose
General molecular biology		
QIAquick® PCR Purification	Qiagen	Purification of DNA products from PCR or other enzymatic reactions
QIAprep® Spin Miniprep	Qiagen	Purification of plasmid DNA, up to 20 µg of high-copy plasmid DNA
QIAprep® Spin Midiprep	Qiagen	Purification of plasmid DNA, up to 100 µg of high- or low-copy plasmid DNA
QIAquick® Gel Extraction Kit	Qiagen	Extraction and purification of DNA fragments from agarose gels
NZY Tissue gDNA Isolation Kit	NZYTech	Small-scale preparation of highly pure genomic DNA
RT-PCR		
High Pure RNA Isolation	Roche	Purification of total RNA from cultured cells
Turbo DNA-*free*™	Ambion	Remove contaminating DNA from RNA preparations
Transcriptor High Fidelity cDNA Synthesis	Roche	Reverse transcribe RNA
LightCycler ® 480 SYBR Green I Master	Roche	Hot-start reaction mix for PCR using the LightCycler® 480 System

All other reagents used during this work are listed in Table VI.5.

Table VI.5. Other reagents used in this work.

Reagent	Chemical Formula	Purity (%)	Supplier
Calcium chloride dihydrate	$CaCl_2 \bullet 2H_2O$	99.5	Merck
Crystal violet	NA	NA	Merck
D-(+)-glucose	$C_6H_{12}O_6$	99	Panreac
Di-potassium hydrogen phosphate	K_2HPO_4	99	Carl Roth
Di-sodium hydrogen phosphate heptahydrate	$Na_2HPO_4 \bullet {}^7H_2O$	98	Carl Roth
EDTA disodium salt dihydrate	$C_{10}H_{14}N_2Na_2O_8 \bullet 2H_2O$	99	Carl Roth
Glacial acetic acid	CH_3COOH	100	Merck
Glycerol	$C_3H_8O_3$	85	Merck
Hydrochloric acid	HCl	37	Carlo Erba
Hydrogen peroxide	H_2O_2	33	Sigma
L-glutathione reduced	$C_{10}H_{17}N_3O_6S$	98	Sigma
Potassium chloride	KCl	99.5	Carl Roth
Potassium dihydrogen phosphate	KH_2PO_4	99.5	Riel-de Haën
Sodium chloride	NaCl	99.5	Fisher Scientific
Sodium hydroxide	NaOH	NA	AkzoNobel Eka
Sodium nitrite	$NaNO_2$	99	Merck
Spermine-NONOate	$C_{10}H_{26}N_6O_2$	98	Sigma
Sucrose	$C_{12}H_{22}O_{11}$	99	Sigma
Tris	$C_4H_{11}NO_3$	99.9	Carl Roth

NA: not applicable
EDTA: Ethylenediamine tetraacetic acid

Stock solutions of 10 mM GSNO (10 mM reduced GSH, 10 mM $NaNO_2$, 0.6 mM HCl) were prepared immediately before use and kept on ice and protected from the light.

Stock solutions of 40 mM spermine-NONOate were prepared in 0.01 M NaOH, aliquoted and stored at – 20 ^{O}C. Aliquots were thawed on ice immediately before use.

VI.4. Digestion and ligation of plasmid DNA and inserts

To produce cohesive ends, the DNA inserts and the plasmid pIMAY were digested with the same restriction endonucleases. To this end, a reaction was set up as described in Table VI.6. The digested products were purified using the QIAquick® PCR Purification kit (Qiagen) and quantified in a Nanodrop ND-1000 UV-visible spectrophotometer (Thermo Fisher Scientific). To ligate the cohesive ends, a reaction was set up as described in Table IV.6. The ligation product was readily used in subsequent transformations, without further manipulation.

Table VI.6. Composition and conditions of the enzymatic reactions for DNA digestion and ligation.

Reagent	Quantity	Reaction Volume (µL)	Incubation
Digestion		50	37 ^{O}C, 2 hours
1st Restriction endonuclease	3.5 µL		
2nd Restriction endonuclease	3.5 µL		
DNA (insert or plasmid)	1.1 µg		
10X NEBuffer	5 µL		
Ligation		20	16 ^{O}C, overnight
10X T4 DNA ligase buffer	2 µL		
Plasmid DNA	50 ng		
Insert DNA	40X moles of plasmid		
T4 DNA ligase	1 µL		

VI.5. Polymerase chain reaction (PCR), colony PCR and real-time quantitative reverse transcription PCR (qRT-PCR)

In vitro amplification of DNA sequences was achieved by polymerase chain reaction (PCR). Depending on the purpose, two different DNA polymerases were used: *Taq* DNA polymerase (New England Biolabs) and Phusion DNA polymerase (Thermo Fisher Scientific). Since the error rate of Phusion DNA polymerase is 50-fold lower than that of *Taq*, this enzyme was used for cloning purposes, whereas *Taq* was used for all other purposes, including colony PCR. The standard PCR master mixes and PCR programs used for each DNA polymerase are listed in Tables VI.7-10. The mix of dNTPs used was purchased from Enzymatic.

Table IV.7. Composition of the PCR master mix used for *Taq* DNA polymerase.

Component	Volume (µL) for a 30 µL reaction	Final Concentration
10X Standard *Taq* reaction buffer	3	1X
10 mM dNTPS	0.6	200 µM
10 µM oligonucleotide foward	2.5	0.8 µM
10 µM oligonucleotide reverse	2.5	0.8 µM
Template DNA	Variable	NA
Taq DNA polymerase	0.3	0.05 units/µL
Nuclease-free water	to 30	NA

Table VI.8. Composition of the PCR master mix used for Phusion DNA polymerase.

Component	Volume (µL) for a 50 µL reaction	Final Concentration
Nuclease-free water	To 50	NA
5X Phusion HF buffer	10	1X
10 mM dNTPs	1	200 mM
10 µM oligonucleotide forward	2.5	0.5 µM
10 µM oligonucleotide reverse	2.5	0.5 µM
Template DNA	Variable	NA
Phusion HF DNA polymerase	0.5	0.02 units/µL

Table VI.9. Standard PCR program for *Taq* DNA polymerase.

Cycle Step	Temperature (^{O}C)	Time (mm:ss)	Cycles
Initial denaturation	95	03:00	1
Denaturation	95	00:45	
Annealing	50 - 60	00:45	30
Extension	68	1 min/kb	
Final extension	68	05:00	1

Table VI.10. Standard PCR program for Phusion DNA polymerase

Cycle Step	Temperature (^{O}C)	Time (mm:ss)	Cycles
Initial denaturation	98	00:30	1
Denaturation	98	00:10	
Annealing	50 - 60	00:30	30
Extension	72	30 sec/kb	
Final extension	72	05:00	1

Upon genetic manipulation, colonies were screened through colony PCR. For this, a small amount of cells was peaked and touched to the side of a PCR tube and microwaved at 80% potency (approximately 800 W), for 7 minutes. The tube was kept on ice until PCR was performed, as described above.

For real-time quantitative reverse transcription PCR assays, the PCR program described in Table IV.11 was used.

Table IV.11. Real-time quantitative reverse transcription PCR program.

Step	Temperature (^{O}C)	Time (mm:ss)	Cycles	Rate
Pre-incubation	95	05:00	1	4.4
Amplification	95	00:10	45	4.4
	55	00:10		2.2
	72	00:10		4.4
Melting Curve	95	00:05	1	4.4
	65	01:00		2.2
	97	Continuous		0.11

VI.6. Agarose gel electrophoresis

Electrophoresis of DNA or RNA samples was performed in agarose gels of either 1 or 2%, stained with SYBR™ Safe DNA Gel Stain (Invitrogen). Electrophoresis was performed in TAE 1X (1 mM EDTA, 20 mM CH_3COOH, 40 mM Tris), at 80 V, in general for 30 minutes, using a Bio-Rad PowerPac™ 300 power supply. At the end, the gels were visualized on an UV transilluminator (Ultra Lum), coupled to the Kodak electrophoresis documentation and analysis system 120.

VI.7. Preparation and transformation of competent cells

VI.7.1. *Escherichia coli* DC10B

Competent cells of *E. coli* DC10B were prepared by the calcium chloride method [74]. An overnight culture of *E. coli* DC10B grown in LB was diluted 1:100 in 20 mL of LB and incubated at 37 ^{O}C and 150 rpm, until an OD_{600} of 0.5. Aliquots of 1 300 µL were pelleted at 5 000 *x*g, for 5 minutes, at room temperature. Pellets were resuspended in 750 µL of sterile, ice-cold, 100 mM $CaCl_2$ and incubated on ice for 1 hour. Cells were harvested again in the same conditions and resuspended in 100 µL of sterile, ice-cold, 100 mM $CaCl_2$. After 1 hour of incubation on ice, the cells were immediately transformed, through the heat shock method [95]. For this, the competent cells were incubated with the DNA of interest, on ice, for 30-45 minutes. The cells were then heat-pulse at 42 ^{O}C for 45 seconds and incubated on ice again for 2 minutes. Upon addition of 900 µL of LB, the cells were incubated at 37 ^{O}C and 150 rpm for 1 hour. Cells were harvested at 5 000 *x*g for 5 minutes at room temperature. The cell pellet was resuspended in 100 µL of its own supernatant, plated on TSA containing chloramphenicol 15 µg mL^{-1} and incubated at 37 ^{O}C overnight.

VI.7.2. *Staphylococcus aureus* RN4220

Competent cells of *S. aureus* RN4220 were prepared by the sucrose method [96]. An overnight culture of *S. aureus* RN4220, grown in TSB, was diluted 1:50 in 100 mL of fresh TSB and incubated at 37 ^{O}C and 150 rpm, until and OD_{600} of 0.4 – 0.6. Cells were harvested at 8 000 *x*g for 10 minutes at 4 ^{O}C, and resuspended in 100 mL of sterile, ice-cold 0.5 M sucrose. This step was repeated two more times with 50 mL and 0.4 mL of sterile, ice-cold 0.5 M sucrose. Cells were aliquoted, flash frozen in liquid nitrogen and stored at – 80 ^{O}C until needed.

For transformation [96], the electrocompetent cells were thawed on ice and incubated with the recombinant plasmids pIMAY-*ric*500, pIMAY-*hmp*500 and pIMAY-*hmp*800, isolated from *E. coli* DC10B, on ice, for 5 minutes. The cells were pulsed at 2.5 kV and 2.5 ms, in an ice-cold, 1 mm electroporation cuvette. After addition of 800 µL of SMMP medium, the cells were incubated at 28 ^{O}C and 200 rpm for 1 hour. Cells were harvested at 5 000 *x*g for 5 minutes at room temperature. The pellet was resuspended in 100 µL of the supernatant and plated on TSA containing chloramphenicol 10 µg mL^{-1}. The plates were incubated at 28 ^{O}C overnight.

VI.7.3. *Staphylococcus epidermidis*

S. epidermidis competent cells were prepared and electroporated as described by M. Grosser and A. Richardson, with small alterations [97]. Briefly, an overnight culture of *S. epidermidis*, grown in TSB, was diluted 1:100 in 50 mL of fresh TSB and incubated at 37 ^{O}C and 150 rpm, to an OD_{600} of 0.8. Cells were harvested at 5 000 *x*g for 15 minutes at 4 ^{O}C, and resuspended in 50 mL of sterile, ice-cold, 10% glycerol. This step was repeated three more times with 25, 2.5, and 1 mL of sterile, ice-cold, 10% glycerol. Cells were aliquoted and electroporated immediately, or flash frozen in liquid nitrogen and stored at – 80 ^{O}C until its utilization.

For transformation, the electrocompetent cells were incubated with the recombinant plasmids pIMAY-*hmp*500, pIMAY-*hmp*800 and pIMAY-*ric*, isolated from *E. coli* DC10B or *S. aureus* RN4220, at room temperature for 30 minutes. The cells were pulsed at 1.0 kV and 2.5 ms, in an ice-cold electroporation cuvette of 1 or 2 mm. After addition of 500 µL of SMMP medium, the cells were incubated at 28 ^{O}C and 200 rpm for 4 hours. Cells were harvested at 5 000 *x*g for 5 minutes at room temperature. The pellet was resuspended in 100 µL of the supernatant and plated on TSA containing chloramphenicol 10 µg mL^{-1}. The plates were incubated at 28 ^{O}C overnight.

VI.8. DNA isolation

VI.8.1. Isolation of plasmid DNA

Isolation of pIMAY from cultured cells (*E. coli* or *S. aureus* RN4220) was achieved using either the QIAprep® Spin Miniprep or the QIAprep® Spin Miniprep kits (Qiagen). The Miniprep kit enables the isolation of up to 20 µg of high-copy plasmid DNA, whereas the Midiprep kit enables the isolation of up to 100 µg of high- or low-copy plasmid DNA. *E. coli* DC10B harboring pIMAY was grown in LB supplemented with chloramphenicol 15 µg mL^{-1}, at 37 ^{O}C and 150 rpm overnight, whereas *S. aureus*

RN4220 was grown in TSB supplemented with chloramphenicol 10 µg mL^{-1}, at 28 ^{O}C and 150 rpm overnight.

In both cases, cells were harvested at 6 000 *x*g, for 15 minutes, and cell lysis was done as indicated by the manufacturer. For the procedure with the Miniprep kit, the plasmid DNA was collected at 16 000 *x*g, for 10 minutes. The supernatant was loaded onto the kit column and the manufacturer's instructions were also followed. For the Midiprep kit, the plasmid DNA was collected at 20 000 *x*g for 30 minutes. The supernatant was centrifuged again at 20 000 *x*g for 15 minutes. The resulting supernatant was loaded onto a QIAGEN-tip 100. The quality and concentration of the isolated plasmid DNA were assessed in a Nanodrop ND-1000 UV-visible spectrophotometer (Thermo Fisher Scientific).

VI.8.2. Isolation of genomic DNA

Genomic DNA (gDNA) was isolated from *S. epidermidis* RP62A with the NZY Tissue gDNA Isolation Kit (NZYTech), with minor modifications to the supplier's protocol. *S. epidermidis* was grown in TSB, at 37 ^{O}C and 150 rpm overnight. Cells were harvested at 8 000 *x*g for 5 minutes, resuspended in 25 µL of 50 mM Tris-HCl pH 8, and lysed by incubation with lysostaphin (1 mg mL^{-1}, 25 µL), at 37 ^{O}C for 45 minutes. Lysates were centrifuged at 13 000 *x*g for 2 minutes, and the supernatants were loaded onto NZYSpin tissue columns, followed by DNA cleanup and elution experiments. The isolated gDNA was analyzed and quantified in a Nanodrop ND-1000 UV-visible spectrophotometer (Thermo Fisher Scientific), and stored at 4 ^{O}C.

VI.8.3. Extraction of DNA from agarose gels

DNA fragments for subsequent cloning procedures were extracted from agarose gels using the QIAquick Gel Extraction Kit (Qiagen), as indicated by the supplier. Briefly, the DNA fragments were excised from the gels using a sharp scalpel, and the gels slices were completely dissolved in Buffer QG, at 50 ^{O}C. After addition of one volume of isopropanol, the mixture was applied to QIAquick columns and centrifuged at 17 000 *x*g for 1 minute. The cleanup steps were performed as described by the supplier. DNA was eluted with Buffer EB and analyzed by gel electrophoresis and in a Nanodrop ND-1000 UV-visible spectrophotometer (Thermo Fisher Scientific).

VI.9. Confirmation of *S. aureus* JE2 NARSA mutants

The presence of the transposon mutations of the strains *S. aureus* JE2 *hmp*::Tn and *S. aureus* JE2 *ric*::Tn was confirmed by PCR as described by the supplier. For this, transposon-specific oligonucleotides were used in combination with those specific for the *S. aureus* JE2 genes, as outlined in Figure VI.1.

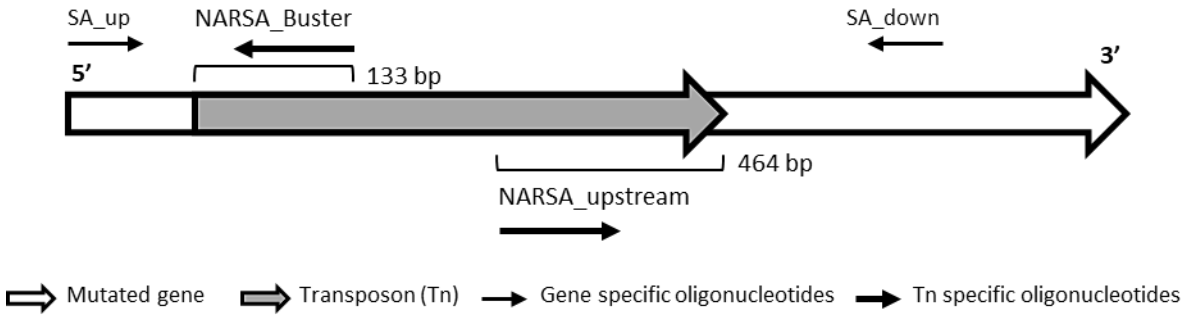

Figure VI.1. Scheme of the pair of oligonucleotides used to confirm the *S. aureus* JE2 transposon mutants from NARSA. The oligonucleotides NARSA_buster and NARSA_upstream anneal with the *bursa aurealis* transposon, while SA_up and SA_down represent oligonucleotides that anneal with the *S. aureus* JE2 chromosome. The expected PCR product size is calculated by the sum of the distance from the annealing site of the gene-specific oligonucleotide to the Tn insertion site, and the distance from the Tn insertion site to the annealing site of the Tn-specific oligonucleotide, which is 133 bp for NARSA_buster and 464 bp for NARSA_upstream.

The PCR products thus obtained were analyzed by gel electrophoresis (Figure VI.2).

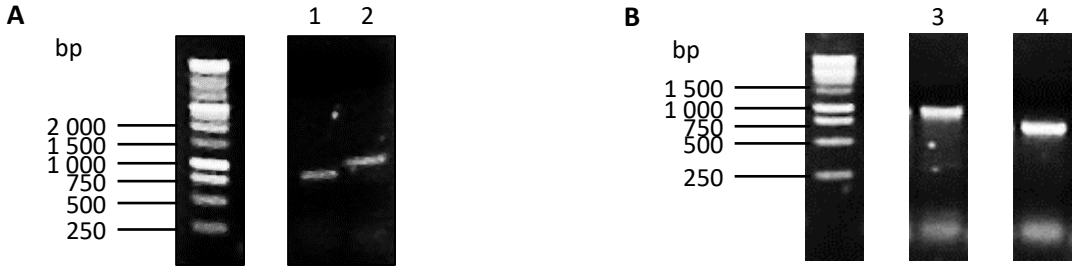

Figure VI.2. Confirmation of *S. aureus* JE2 *hmp*::Tn and *ric*::Tn mutations. (A) The mutation of *S. aureus* JE2 *hmp*::Tn was confirmed using the pairs of oligonucleotides (1) NARSA_upstream/SA_hmp_down and (2) NARSA_buster/SA_hmp_up. The expected size of the amplicons is 964 and 977 bp, respectively. (B) The mutation of *S. aureus* JE2 *ric*::Tn was confirmed using the pairs of oligonucleotides (3) NARSA_buster/SA_ric_up and (4) NARSA_upstream/SA_ric_down. The expected size of the amplicons is 1 079 and 688 bp, respectively. Electrophoresis was performed in 1% agarose gels, at 80 V.

VI.10. Creation of unmarked deletion mutations by allelic replacement mutagenesis

In 2012, Monk and colleagues described a protocol for the creation of unmarked deletion mutations in *S. aureus* and *S. epidermidis*, done by allelic replacement mutagenesis [74]. This protocol makes uses of a new cloning strain, *E. coli* DC10B, and a new allelic replacement vector, pIMAY (Figure VI.3), developed by the authors, and emerged in response to the difficulty experienced in transforming *S. epidermidis*.

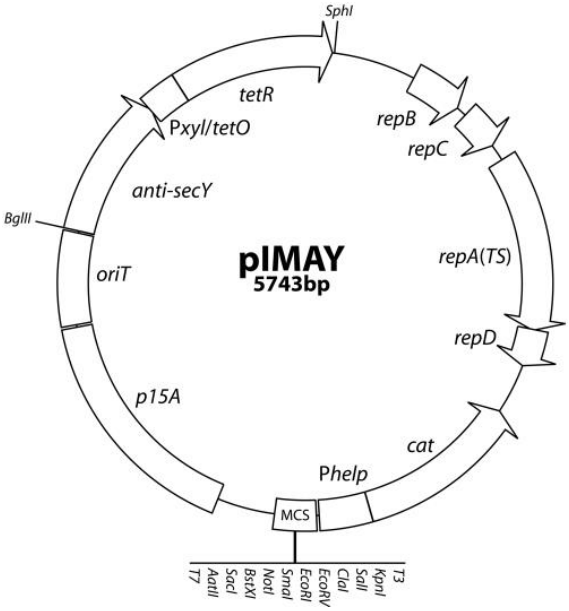

Figure VI.3. Genetic map of pIMAY. The plasmid pIMAY is a low-copy-number *E. coli*/staphylococcal shuttle temperature-sensitive plasmid, which was designed for the construction of *S. aureus* and *S. epidermidis* mutants [74]. The restriction sites listed are unique. It includes p15A, low-copy-number *E. coli* origin of replication; *oriT*, origin of transfer for conjugation; *anti-secY*, tetracycline-inducible antisense *secY*; P*xyl,* xylose promoter; *tetO*, tetracycline operator; *tetR*, tetracycline repressor for tetracycline resistance; *repBCAD*, temperature-sensitive replicon for Gram-positive bacteria; *cat*, chloramphenicol acetyltransferase for chloramphenicol resistance; MCS, multiple cloning site.

The allelic replacement mutagenesis protocol is outlined in Figure VI.4. Briefly, the upstream and downstream flanking regions (~500 bp each) of the gene to be deleted were PCR-amplified, combined by splicing by overlap extension PCR (SOE-PCR) and cloned into pIMAY. The recombinant plasmid was transformed into *E. coli* DC10B, to bypass cytosine methylation, and later electroporated into the target *Staphylococcus*. Transformants were selected on BHIA containing chloramphenicol 10 µg mL^{-1}, at 28 ^{O}C, which is a permissive temperature for pIMAY.

To induce integration of pIMAY into the chromosome, a colony from the transformation plate was inoculated into BHI supplemented with chloramphenicol 10 µg mL^{-1}, and grown overnight at 37 ^{O}C, which is a non-permissive temperature for pIMAY. Afterwards, cells were serially diluted in PBS and plated on BHIA containing chloramphenicol 10 µg mL^{-1}. The resulting colonies were screened by colony PCR for the absence of the extrachromosomal plasmid, using oligonucleotides specific for the MCS of pIMAY, followed by another colony PCR to assess whether plasmid integration occurred upstream or downstream of the gene.

Clones from either upstream or downstream integration events, free of replicating plasmid, were then inoculated into BHI at 28 ^{O}C overnight, and plated on BHIA containing anhydrotetracycline 1 µg mL^{-1}, at 28 ^{O}C

for two days. Anhydrotetracycline induces the expression of the *secY* antisense RNA, which inhibits growth of the clones maintaining the replicative plasmid. The resulting colonies were streaked on BHIA containing anhydrotetracycline 1 µg mL^{-1} and BHIA containing chloramphenicol 10 µg mL^{-1}, at 37 ^{O}C overnight. Chloramphenicol-sensitive colonies were further screened by colony PCR to identify clones with the desired mutation, which were later validated by PCR amplification of genomic DNA flanking the deletion and DNA sequencing.

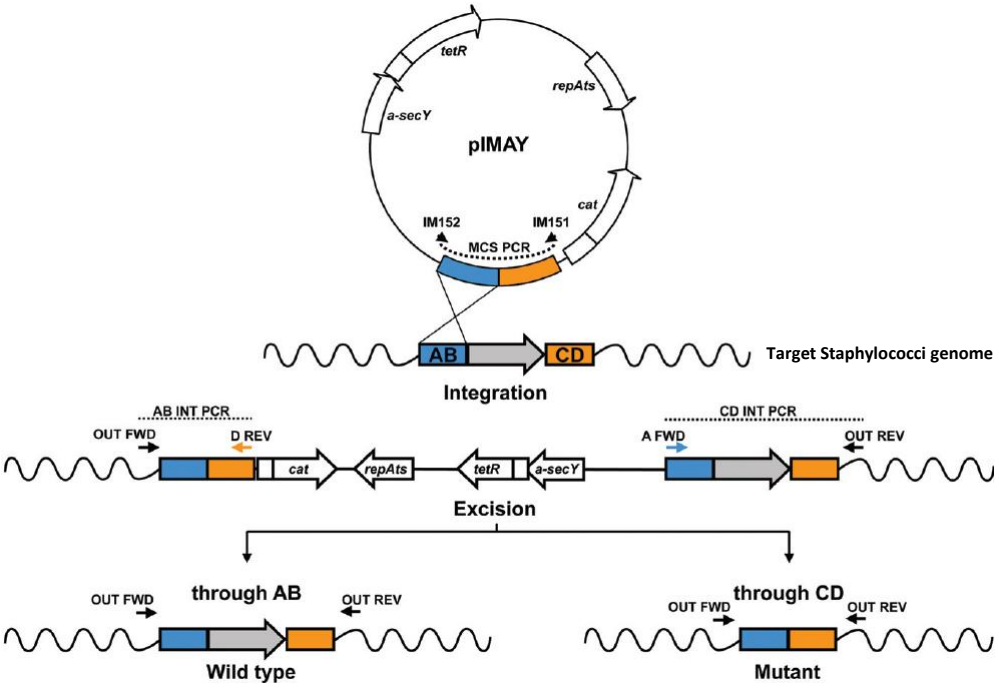

Figure VI.4. Allelic replacement with pIMAY [74]. The recombinant plasmid is isolated from *E. coli* DC10B and electroporated into staphylococci at 28 ^{O}C, a permissive temperature for pIMAY. Integration of the plasmid into the staphylococci chromosome is stimulated by growth at 37 ^{O}C, a non-permissive temperature for pIMAY, in the presence of chloramphenicol. Loss of the replicating plasmid is screened by colony PCR with oligonucleotides specific for the MCS of pIMAY (IM151/IM152). Clones without the replicating plasmid are further screened for the side of integration with a combination of chromosomal (OUT FWD, OUT REV) and cloning (D REV, A FWD) oligonucleotides. The scheme represents an integration event through the AB side. Clones from either AB or CD integration events are grown at 28 ^{O}C, without antibiotic selection, to stimulate rolling circle replication, and then plated on TSA containing anhydrotetracycline 1 µg mL^{-1}. Anhydrotetracycline induces the expression of the *secY* antinsense RNA, which inhibits growth of cells maintaining the plasmid. Plasmid excision through the AB side re-creates the wild-type locus, while CD excision yields a mutated gene.